SEARS FOUNDATION FOR MARINE RESEARCH
BINGHAM OCEANOGRAPHIC LABORATORY, YALE UNIVERSITY

JOURNAL OF MARINE RESEARCH

VOLUME I, 1937-38

NUMBER 3

ISSUED SEPTEMBER 20, 1938, NEW HAVEN, CONN., U. S. A.

JOURNAL OF MARINE RESEARCH

PUBLISHED BY

SEARS FOUNDATION FOR MARINE RESEARCH
BINGHAM OCEANOGRAPHIC LABORATORY, YALE UNIVERSITY

BOARD OF EDITORS

C. G. ROSSBY
Massachusetts Institute of Technology

THOMAS G. THOMPSON
Oceanographic Laboratories University of Washington

H. U. SVERDRUP
Scripps Institution of Oceanography

A. E. PARR
Bingham Oceanographic Laboratory Yale University

MANAGING EDITOR

A. E. PARR
Bingham Oceanographic Laboratory
Yale University
New Haven, Conn.

ASSISTANT: *D. T. Pitcher*

Funds sufficient for the annual printing and distribution of about 200 pages of this Journal have been made available from the income of the Sears Foundation for Marine Research of Yale University for the current year, and it is intended that this contribution shall be continued on a permanent basis, with the income derived from subscriptions to be used solely to increase the volume and improve the quality of the Journal for the benefit of its subscribers and contributors.

The Journal will be issued in three numbers per year, beginning with 1938. Volume I also contains the presubscription number (Vol. I, No. 1) issued in November, 1937.

Subscription price three dollars per year. Address all communications to the managing editor.

SEARS FOUNDATION FOR MARINE RESEARCH
BINGHAM OCEANOGRAPHIC LABORATORY, YALE UNIVERSITY

JOURNAL OF
MARINE RESEARCH

VOLUME I 1937–1938 NUMBER 3

RADIUM CONTENT OF SOME INSHORE BOTTOM SAMPLES IN THE PACIFIC NORTHWEST

By

C. L. UTTERBACK AND L. A. SANDERMAN

Physics and Oceanographic Laboratories, University of Washington, Seattle

The radium content of ordinary rock formations is quite well established and has been summarized by Jefferys (*3*). However, a comparatively few radium determinations have been made on samples taken from the ocean bottom. Joly (*4*) has reported twelve radium determinations of surface samples collected from the Atlantic and Pacific Oceans. Pettersson (*5*) has reported on determinations made on twenty-eight samples, most of them taken from the Atlantic Ocean, while Piggott (*6*) has reported on twenty-eight samples taken largely from the Pacific Ocean. Evans (*1*) has reported on one sample taken from off the Coast of California.

For several years the authors have been conducting a rather extensive survey of the radium content of both surface bottom and core samples taken along the Pacific Coast of Alaska, Canada, and the northern part of the United States. Considerable work has also been done on samples from the Bering Sea, Bering Strait, and off the Arctic Coast of Alaska. This report is a preliminary one on surface bottom samples involving the region of the San Juan Archipelago and Vancouver Island.

The method and apparatus used for the determination of the radium content is essentially that developed by Evans (*2*). For the sake of completeness a brief description of the method is given. A schematic diagram of the apparatus is shown in Figure 72.

The radium content of a sample is determined by removing the radon which is in equilibrium with the radium in a sample and then measuring the ionization produced by the radon in a double ionization chamber by means

of a string electrometer. The sample is dried and ground to pass through a sixty mesh screen. It is then sampled, weighed, and baked in a furnace for one hour at 900° to 1000° C. to remove carbonates, organic matter, or water of crystallization, after which it is sealed in a glass tube and allowed to stand for twenty-eight days or more to insure equilibrium between the radium and the radon.

When a determination is to be made, the free radon from the previously heated sample is temporarily stored in the reservoir (B). The sample is placed in the graphite crucible vacuum electric furnace (A). The system (A, C, E) is then evacuated. After evacuation of the system, the crucible

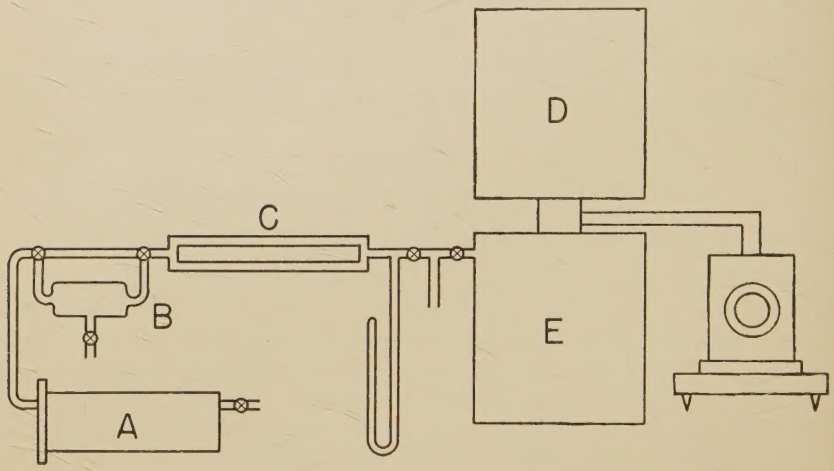

Figure 72. Schematic diagram of the apparatus.

is heated to approximately 2000° C. which completely removes the radon. This, together with the radon in the reservoir (B), is swept through the ion trap (C) into the ionization chamber (E) by means of radon-free nitrogen. The potentials of the two chambers are such that the electrometer measures only the difference in ionization in the chambers. Since one of the chambers (E) contains nitrogen and radon while the other chamber (D) contains only nitrogen, the deflection of the string electrometer will depend only upon the ionization current due to the radon. The ionization current was photographically recorded, thus giving a continuous record for a period of twenty-four hours duration. In order to correct for the ionization due to radioactive contamination of the chambers, cosmic rays, etc., each radon measurement was bracketed by background determinations. The apparatus was calibrated with a standard radium solution which was supplied through the kindness of R. D. Evans.

The location of the samples and their radium content, in grams of Ra per gram of dry material, is tabulated in Table I and indicated in the accompanying chart, Figure 73. The diameters of the circles are proportional to the radium content.

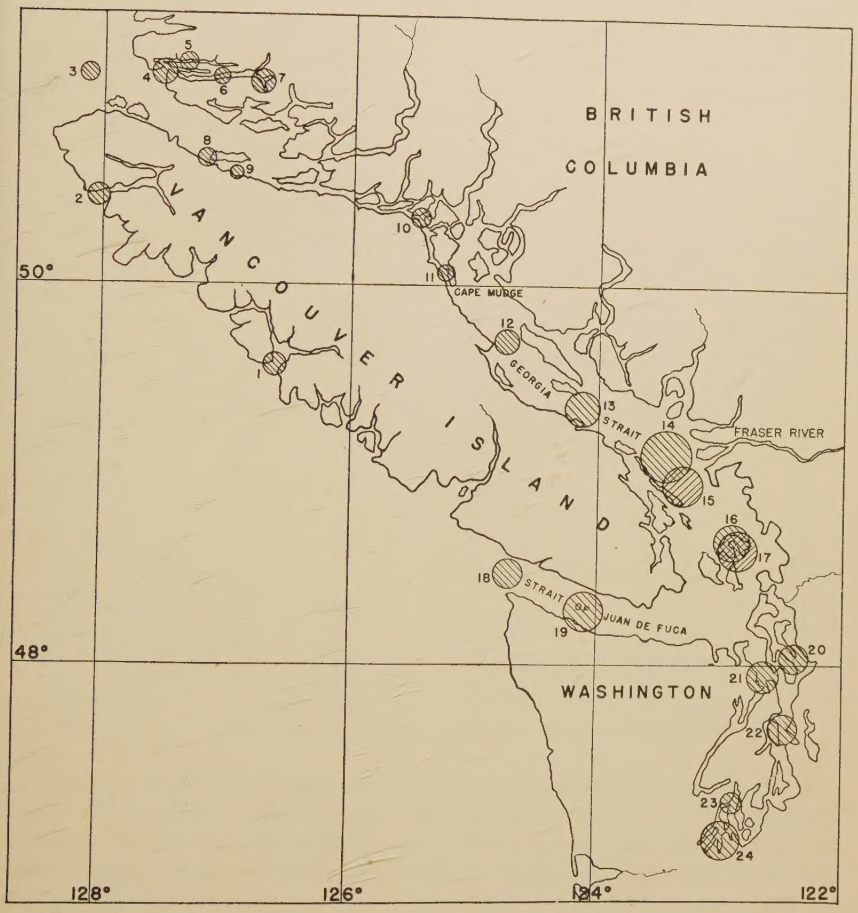

Figure 73. Chart of the San Juan Archipelago and Vancouver Island region. The diameter of the circles is proportional to the radium content.

Stations one to eleven are situated around the northern part of Vancouver Island. The samples from these stations are made up of the sediment from Vancouver Island and from the coast of British Columbia. This territory is composed largely of schist and quartzite with a small amount of diorite.

The average radium content of the eleven stations is 0.24×10^{-12} g. Ra per g. which is in agreement with the radium content of the rock formations of the surrounding territory.

The same may be said to apply to the stations from the Puget Sound area. Samples twenty to twenty-four, inclusive, have an average radium content of 0.37×10^{-12} g. Ra per g. The surrounding territory is largely made up of glacial drift with a radium content comparable with that of the average of the stations.

TABLE I

Location of Stations and Radium Content of Samples

Station	*Latitude*	*Longitude*	*Depth (meters)*	*G. of Ra per g.*	*Description*
1	49°35′ N	126°35′ W	30	$.28 \times 10^{-12}$	Clay
2	50°29′	128°04′	110	.27	Clay
3	51°05′	128°07′	180	.23	Sand
4	51°02′	127°32′	20	.29	Clay
5	51°08′	127°18′	270	.23	Clay
6	51°03′	127°12′	130	.20	Clay
7	51°04′	126°40′	100	.30	Clay
8	50°38′	127°12′	40	.22	Sand
9	50°34′	126°57′	10	.16	Sand
10	50°19′	125°27′	235	.24	Sand
11	50°05′	125°17′	20	.20	Sand
12	49°43′	124°45′	175	.30	Clay
13	49°21′	124°08′	147	.43	Clay
14	49°07′	123°27′	275	.64	Clay
15	48°58′	123°20′	130	.50	Clay
16	48°40′	122°55′	30	.46	Clay
17	48°37′	122°51′	40	.49	Clay
18	48°30′	124°43′	75	.37	Clay
19	48°17′	124°05′	200	.49	Sand
20	48°03′	122°23′	150	.36	Clay
21	47°57′	122°38′	90	.40	Sand
22	47°38′	122°27′	150	.36	Clay
23	47°18′	122°51′	30	.26	Sand
24	47°07′	122°55′	12	.48	Clay

The sediment composing the samples from stations twelve to nineteen is furnished by the Fraser River and the surrounding territory. The flood tide in Georgia Strait enters through the Strait of Juan de Fuca and meets the flood tide entering through Johnston Strait at a point approximately ten miles south of Cape Mudge. Therefore, the stations near the mouth of the Fraser River are composed largely of the sediment from the Fraser River while the stations farther away are composed to a greater extent of the sediment from the surrounding territory.

It is of interest to note that the radium content is relatively high near the mouth of the Fraser River and decreases with some uniformity in Georgia Strait to the north, and also into the Strait of Juan de Fuca to the south and west. The drainage basin of the Fraser River is predominately granitic,

while the southern portion of Vancouver Island and the northern portion of the Olympic Peninsula are made up of sandstone and basalt. Radium content of granite is approximately three times that of sandstone or basalt.

Thus it is evident that the radium content of inshore ocean bottom samples is largely determined by the radium content of the sediment of which the sample is composed. Also it appears that the radium content of the sediment is determined by the radium content of the land area from which the sediment is derived.

It will be noticed that the radium content of all the stations is lower than that of the deep ocean bottom samples as reported by the investigators previously mentioned. Five stations, reported by Piggott (*6*) in the northeast Pacific, have an average of 7.6×10^{-12} g. Ra per g. while the station taken by Evans (*1*), thirteen nautical miles off the southern coast of California, has a value of 3.2×10^{-12} g. Ra per g. The average of all the determinations made by the authors is 0.34×10^{-12} g. Ra per g. The average of the sixteen clay samples is 0.37×10^{-12} g. Ra per g. while that of the eight sand samples is 0.28×10^{-12} g. Ra per g.

The radium content of the samples reported here, which were taken near shore in comparatively shallow water, shows no correlation with depth of water.

REFERENCES

1. Evans, R. D.
1934. Improved Technique for Determination of Radon and Radium in Liquids. Phys. Rev., 46, 328.

2. Evans, R. D.
1935. Apparatus for Determination of Minute Quantities of Radium, Radon, and Thoron in Solids, Liquids, and Gases. Rev. Sci. Inst., 6, 99.

3. Jefferys, H.
1936. Radioactivity of Rocks. Gerlands Beitr. z. Geophys., 47, 149.

4. Joly, J.
1908. On the Radium Content of Deep Sea Sediments. Phil. Mag., 16, 190.

5. Pettersson, Hans
1930. Teneur en Radium des Dépots de Mer Perfonde. Fascicule LXXXI of Resultats de Campagnes Scientifiques par Albert 1er Prince Souverain de Monaco.

6. Piggott, C. S.
1933. Radium Content of Bottom Ocean Sediments. Am. Sci., 35, 229.

TIDES AND TIDAL CURRENTS IN THE GULF OF PANAMA

By

RICHARD H. FLEMING

*Scripps Institution of Oceanography**
University of California
La Jolla, California

The following discussion deals with two specific problems: first, the increase in the range of tide between the entrance and the head of the Gulf of Panama; and second, the variations in the tidal current velocities between the entrance and the head of the Gulf. Both phenomena are shown to be related to the bottom topography. The profile of the bottom across the continental shelf plays an important role in determining the distribution of tidal current velocities in such an area, and the maximum velocities are shown to occur at or near the edge of the shelf. Treating the tide of the Gulf of Panama as a standing wave, the current velocities in the Gulf have been related to the range and phase of the tide. Although the numerical examples are restricted to the Gulf of Panama, the same methods may be applied to other regions.

Range of tide and time of tide in the Central American Pacific.—The average range of tide in the Central American Pacific region is shown in Figure 74. An insert of the Gulf of Panama (Fig. 74A) shows additional tidal data for the stations within the Gulf. These figures were prepared from data in the Tide Tables for the Pacific and Indian Ocean, 1938 (U. S. Coast and Geodetic Survey). The upper value in the insert map is the average range of the tides, the lower value the average range of the spring tides, in feet. The tides are of the semi-diurnal type. The tides in the Gulf of Panama vary from 5 feet at minimum neap tides to over 22 feet at maximum springs (Kirkpatrick, 1926).

In the Central American Pacific area the average tidal range is greatest in the innermost portion of the Gulf of Panama. It decreases to 9 feet along the South American coast and there is a general decrease northward along the Central American coast. The insert map shows that even within the Gulf of Panama there is considerable variation in the average range of the tide. The maximum values for both average and average spring ranges are found at Balboa where the values are 12.6 and 16.4 feet respectively. At the entrance to the Gulf the values on the west side, Cape Mala, are 10.3 and 13.0 and on the east side, Piñas Bay, 10.8 and 13.8 feet. That is, the range of tide at the head of the Gulf is about 2.5 feet greater than at the

* Contributions from the Scripps Institution of Oceanography. New Series, No. 24.

entrance. The values in parentheses (Fig. 74) are the lunitidal intervals expressed in terms of Greenwich Meridian Time for the respective stations. From these it is apparent that the time of tide is almost the same over the

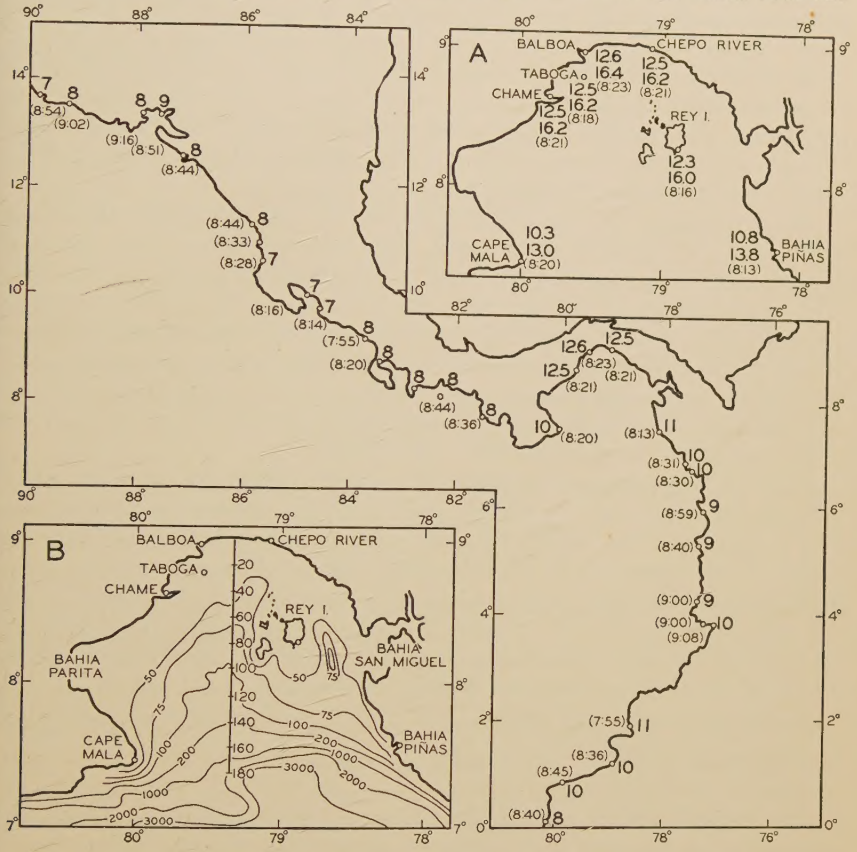

Figure 74. Mean range of tide and the time of tide (G.M.T.) for stations in the Central American Pacific. *Insert* A. Mean range of tide, mean range of spring tides and the time of tide (G.M.T.) in the Gulf of Panama. *Insert* B. Bottom topography of the Gulf of Panama (contour depths in meters), and the location of the section along 79° 20′ W. Distances from the head of the Gulf are given in kilometers.

entire area. The greatest difference in time of tide, in the area shown in this map, is 1 hour 20 minutes. When it is noted that some stations are on the open coast and others in bays and inlets, where the tide will be somewhat retarded, the differences are strikingly small.

As the time of tide is so constant over such a large portion of the coast, it is obvious that the tide in this region must have the character of a standing

wave. Whether this is of the form discussed by Harris or whether it is due to the interference of a series of progressive waves need not concern us at this time. The general form of the coast line of the Pacific coast of the Americas must have an important bearing on the nature of the tides in this area. From Figure 74 it can be seen that the coast forms a large bight approximately semicircular in shape. The Gulf of Panama proper forms a secondary indentation at the head of the bight. Two interesting points arise; first, what causes the greater range in tide at the head of the Gulf and second, why are the ranges along the coast of South America greater than those along the coast of Central and North America?

These questions are undoubtedly associated with the properties of the tidal wave and the form of the coast. The fact that the wave is restricted by the converging coast line will result in an increase in range near the head. The greater range in tide on the southern and eastern coast is probably related to the orientation of the tidal wave and the form of the coast line, although the deflective force of the earth's rotation may play some part. In the Gulf of Panama we must again consider the form of the coast line and the deflective force of the earth's rotation, and a third factor, namely: the shallower depths in the inner part of the Gulf.

Effect of topography on range of tide.—Lamb (1932) discusses the effect of changing depth and boundaries upon the form of tidal waves in canals. If we assume that the Gulf of Panama is of constant breadth but of variable depth we can apply certain equations from Lamb. The depths along a line running from the head of the Gulf to the entrance on the meridian 79° 20′ W (Fig. 74B) are shown in Figure 75, curve I. From this profile it would appear that the slope between the head of the Gulf and a point 120 km from the head could be considered constant. If this is the case, we can use the equation given by Lamb (1932, p. 276) for a canal of constant width but linearly changing depth, that is where $h = h_a \frac{x}{a}$.

The general equation for tidal movements in a canal, disregarding the effect of the rotation of the earth, is given by Lamb (1932, p. 275).

$$\frac{g}{b}\frac{\partial}{\partial x}\left(hb\frac{\partial \eta}{\partial x}\right) + \sigma^2\eta = o \tag{1}$$

where $\eta_a = C \cos(\sigma t + \varepsilon)$.

g = gravitational constant.

b = breadth of the canal.

h = depth at distance x from the end. h_a = depth at distance $x = a$.

η = level of the tide at time t.

C = amplitude of the tide at $x = a$.

$\sigma = \frac{2\pi}{T}$, where T is the tidal period, t some fraction of T and ε some fraction of 2π which is used when it is necessary to correct for phase differences. In the present case it may be disregarded. In the case under consideration b is constant and $h = h_a \frac{x}{a}$. Therefore,

$$\frac{\partial}{\partial x}\left(x \frac{\partial \eta}{\partial x}\right) + k\eta = o, \text{ where } k = \frac{\sigma^2 a}{g h_a}. \tag{2}$$

The solution can be written as a Bessel function.

$$\eta = \frac{J_o(2k^{1/2} x^{1/2})}{J_o(2k^{1/2} a^{1/2})} C \cos(\sigma t). \tag{3}$$

Only the first three terms of the expansion need be considered and if we omit $C \cos(\sigma t)$ we may write

$$\eta = \frac{1 - (1/2.2k^{1/2}x^{1/2})^2 + 1/4(1/2.2k^{1/2}x^{1/2})^4}{1 - (1/2.2k^{1/2}a^{1/2})^2 + 1/4(1/2.2k^{1/2}a^{1/2})^4} \cdots.$$

In this case $a = 120 \times 10^3$ m, $h_a = 120$ m, and, considering a semi-diurnal tide, $T = 4.48 \times 10^4$ sec. Therefore:

$$k = 2.00 \times 10^{-6}.$$

If we solve for the value of η when $x = o$, that is, at the head of the Gulf and reintroduce the term $C \cos(\sigma t)$:

$$\eta_o = 1.30\ C \cos(\sigma t).$$

That is, the range in tide at the head of the Gulf should be 30% greater than at the entrance. Actually the difference is much less than this and consequently we must find some other expression that gives a better agreement. From a study of the profiles of other shelves and from other sections in the Gulf, it appeared that a parabolic curve more nearly approximated the profile of the bottom. The expression for the bottom profile could then be written $h = h_a \sqrt{\frac{x}{a}}$. This curve fitted to $h_a = 120$ m and $a = 120$ km is shown in Figure 75, curve II. The parabolic curve gives depths somewhat greater than the actual depths of the section in the inner portion of the Gulf. In this case b is constant and $h = h_a \sqrt{\frac{x}{a}}$, consequently

$$\frac{\partial}{\partial x}\left(\sqrt{x} \frac{\partial \eta}{\partial x}\right) + k\eta = o. \quad k = \frac{\sigma^2 \sqrt{a}}{g h_a} = 5.77 \times 10^{-9}. \tag{4}$$

The solution can again be written as a Bessel function which expanded yields

$$\eta = \frac{1 - \frac{2}{3} kx^{3/2}}{1 - \frac{2}{3} ka^{3/2}} \ldots . C \cos (\sigma t). \tag{5}$$

At the head of the Gulf, where $x = o$,

$$\eta_o = 1.19\ C \cos (\sigma t). \tag{6}$$

That is, on these assumptions the range of tide at the head of the Gulf should be 1.19 times greater than that off the entrance to the Gulf. At Piñas Bay on the eastern side of the mouth of the Gulf, where the shelf is very narrow, the average range of tide is 10.8 feet and the average spring range is 13.8 feet. At Cape Mala, on the western side of the entrance to the Gulf, the average ranges are 10.3 and 13.0 feet respectively. As the differences between Cape Mala and Piñas Bay may be due to the effect of the earth's rotation, we may assume that the average ranges in tide at the central part of the entrance to the Gulf are about 10.5 feet and 13.4 feet. If we multiply these values by 1.19 we obtain 12.5 feet and 16.0 feet for the averages of the tide at the head of the Gulf. At Balboa the actual values are 12.6 feet and 16.4 feet.

If we adjust the theoretical average tidal amplitude so that it agrees with the observed amplitude at Balboa, we obtain the curve shown in Fig. 75, curve IV. The amplitude of the tide which was computed by considering the slope of the bottom as constant is also shown (curve III). The apparent contradiction in the results obtained, namely that the bottom profile is almost a straight line and that the tidal range at the head of the Gulf is much smaller than would be expected from this, is undoubtedly due to the effect of friction. This is the reason why the parabolic function which gives depths greater than the actual profile yields an expression for the tidal amplitude which agrees more closely with the actual conditions. The fact that the parabolic function gives such a good agreement at Balboa must then be considered as more or less accidental. The average amplitudes at the various stations in the Gulf are also shown and, although the agreement with the parabolic expression is good near the head of the Gulf, it does not fit very well for Rey Island. In this case the value obtained using the straight line function is somewhat closer. In order to facilitate calculations the parabolic expression for the tidal amplitude has been used in the following discussion.

Characteristics of tidal currents.—In a study of the oceanographic conditions in any area the horizontal water movements associated with the rise and fall of the tide are usually of much greater significance than the vertical movements. The tidal range in the Gulf of Panama is large and it is obvious that associated with the tides there must be strong tidal currents. Tre-

mendous volumes of water must enter and leave the Gulf during each tidal period. There are many references to the strong tidal currents in the Gulf of Panama (over 1 knot in many instances) in the Coast Pilots and the

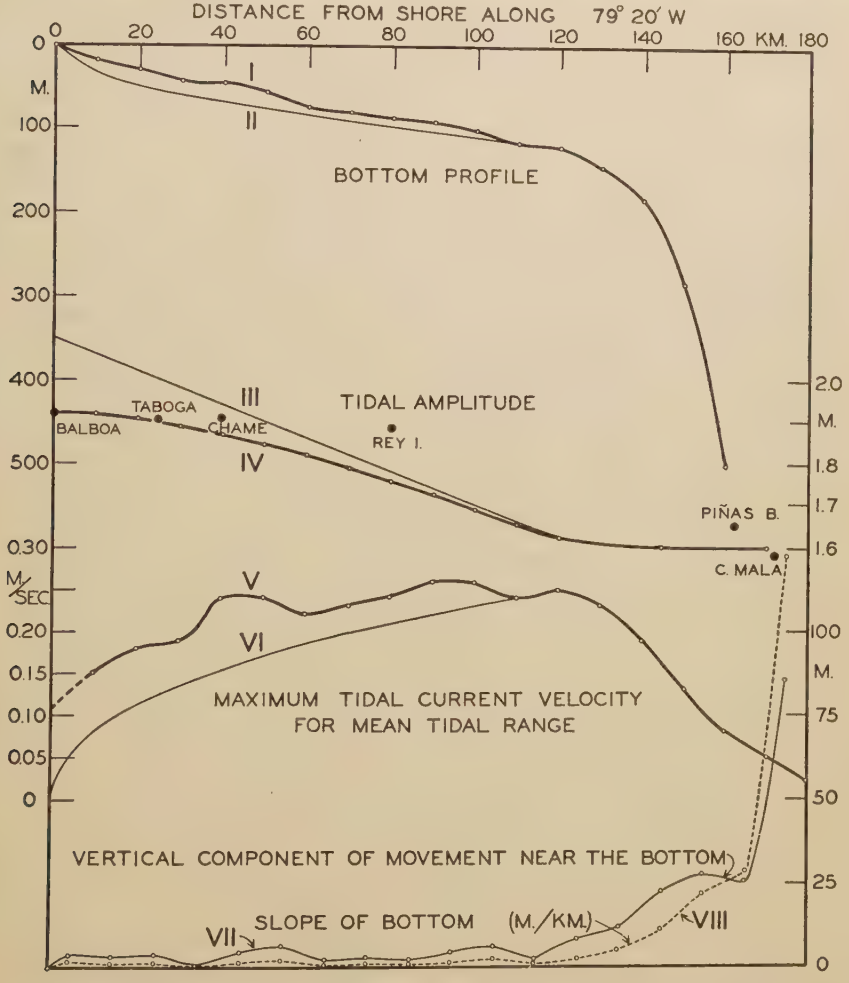

Figure 75. Bottom profile along 79° 20′ W. in the Gulf of Panama, the mean amplitude of the tide along this section, the maximum current velocities for the mean amplitude of the tide and the vertical movements near the bottom.

newer charts published by the United States Hydrographic Office, particularly in the region of the Perlas Islands Archipelago (U. S. Hydrographic Office Charts No. 1019, 1410, 5580, 5584, etc.).

As the tidal range in the Gulf of Panama varies from 5 feet to over 22 feet there must be wide variations in the maximum velocities. This may account, in part at least, for the many statements that the Gulf is an area of extremely variable currents. Also, as the tidal currents will reach maximum velocities twice during the tidal period of about 12.5 hours, and approach zero velocities twice during the same period it is obvious that the movements in the Gulf will be very variable. Although the tidal currents may reach high velocities, they are reversing currents and therefore bring about no actual transport of water, consequently their effect upon the oceanographic conditions can only be that of mixing of the waters already present. The point which must be emphasized is that the non-tidal circulation which determines the general oceanographic features in the Gulf is probably rather steady over relatively long periods and that the currents reported as variable are associated with the tides. They are of a periodic nature and depend upon the phase and range of the tide.

It has been shown in the preceding section that the tides in the Central American region and in the Gulf of Panama can be treated as standing waves. Therefore the maximum current velocities will be found at half tide. Certain other factors must be taken into consideration, such as the effect of the earth's rotation and the effect of the bottom configuration. In the absence of the effect of the rotation of the earth the horizontal movement of a particle associated with the tides would be in a straight line oscillating back and forth. However the effect is such that any particle in motion tends to be deflected to the right of the direction of progress in the northern hemisphere and to the left in the southern hemisphere. Only on the equator is this effect zero and there the tidal currents should be rectilinear. The effect increases as the sine of the latitude and consequently the tidal currents are not rectilinear but trace ellipses of increasing width as the latitude increases until at the poles the movements will be circular. One ellipse will be completed in each tidal period.

The relationship of maximum and minimum velocities under a given set of conditions in the open ocean is that:

$$S = \frac{V_{min}}{V_{max}} = 2 \sin \varphi \frac{T}{T'}$$

when T = the period of the tide, $T' = 24$ hours and φ = latitude.

For a semi-diurnal tide, T is approximately equal to $\frac{1}{2}T'$.

Therefore, $$S \approx \sin \varphi.$$

For the lower latitudes the values of S are given in the following table:

Latitude	*S*	*V max.*
5°	.091	11.0 × *V min.*
6°	.108	9.3 × *V min.*
7°	.127	7.9 × *V min.*
8°	.145	6.9 × *V min.*
9°	.163	6.1 × *V min.*
10°	.180	5.6 × *V min.*

From the above figures it can be seen that the effect of the earth's rotation upon tidal currents must be slight in the Central American region as the maximum velocities will be many times as great as the minimum velocities. In the Gulf of Panama, itself, there is undoubtedly some effect but it will be so slight compared to the flow in and out of the Gulf that we need not give it much consideration. Furthermore the proximity to land will result in the development of gradients which will tend to reduce the lateral deflection. However, it should be emphasized that the tidal currents will at no time be zero; but will instead decrease to minimum velocities at high and low water.

Tidal currents over the continental shelf.—As stated above, the topography of the bottom has an important role in determining the velocity of tidal currents. It is not the depth alone which enters when we are considering the water movements associated with a standing wave; but also the relationship of the depth and the distance from shore.

Let us examine the case where a standing wave is oriented at right angles to the coast line and where the level at the tide of time t and point x is represented by

$$\eta = C_x \cos(\sigma t)$$

where C_x is the amplitude of the tide at the point x. Substituting for η, in equation (1) we obtain

$$\frac{\partial}{\partial x}\left(h\frac{\partial \eta}{\partial x}\right) = -\frac{\sigma^2}{g} C_x \cos(\sigma t).$$

$$g\frac{\partial \eta}{\partial x} = -\frac{\sigma^2}{h}\cos(\sigma t)\int_o^x C_x\, dx.$$

Now
$$\frac{\partial u}{\partial t} = -g\frac{\partial \eta}{\partial x}.$$

(7) Therefore
$$\frac{\partial u}{\partial t} = \frac{\sigma^2}{h}\cos(\sigma t)\int_o^x C_x\, dx.$$

(8) and
$$u = \frac{\sigma}{h}\sin(\sigma t)\int_o^x C_x\, dx.$$

From this we see that the velocity will vary inversely as the depth (h) at the point x and directly as the volume of water represented by the integral of the level of the tide over the distance from the shore to the point x. If the level of the tide was constant, this would merely represent the product of the level of the tide and the distance x.

Let us examine the velocity of the tidal currents over shelves of certain types. If we consider only the maximum velocities, that is when $\sin(\sigma t) = 1$, then,

$$u_{max} = \frac{\sigma}{h} \int_o^x C_x \, dx. \tag{9}$$

Let us further assume that C_x is constant, then

$$u_{max} = \frac{\sigma}{h} Cx.$$

Certain striking relationships can then be readily seen. First: if the depth is constant, the velocity will vary as the distance from shore. Second: if the slope is constant and passes through $x = o$, that is $\frac{x}{h}$ is constant, then the velocity is constant and independent of x. Third: if the slope is constant over a certain stretch of the shelf, the velocity over that stretch will decrease on approaching the coast if the slope is $< \frac{h}{x}$ but $>$ horizontal, and will increase if the slope is $> \frac{h}{x}$. Fourth: the velocity will be maximal where $\frac{x}{h}$, that is the distance from shore divided by the depth, is greatest.

The last mentioned point is one of general interest because of the characteristic form of the continental shelves. Although the width of the continental shelf varies greatly from place to place along the coasts it has, in practically all cases, a zone of relatively constant depths before reaching the continental slope. Consequently the value of $\frac{x}{h}$ is greatest at or near the edge of the shelf, and therefore the tidal currents will attain their maximum velocities in this zone, provided that the tidal wave is not distorted by the outline of the coast. If we consider the greater range of the tide usually associated with the shoaling bottom, that is when C_x increases as x decreases, the volume of water passing x will be greater than if the amplitude is constant. Consequently the velocities will be greater.

It must be borne in mind that the foregoing considerations were based on certain assumptions, namely, that we had a standing wave oriented at right angles to the coast line. This case is probably not encountered in

very many areas in the ocean. However, the general conception concerning the distribution of velocities over the shelf will hold true whenever there is *any* transport of water across the shelf which is associated with the tidal movements. If the tidal wave is of the progressive type, the maximum velocities will occur at high and low water instead of at half tides as in the standing wave. If the tidal wave is reflected or otherwise affected by the proximity of the coast, the tidal currents may bear some other relation to the tidal cycle.

In the considerations above it has been assumed that the depth was uniform or sloped upwards continuously towards the coast. It has been shown that the velocity at any distance from the coast is a function of the depth at x, and the integral of the amplitude of the tide over the distance x. It should be noted that the depths inside of x have no effect on the velocity at x, except as they may affect the amplitude of the tide.

Tidal current velocities along 79° 20′ W in the Gulf of Panama.—It has been shown that the variations in the amplitude of the tide in the Gulf of Panama can be expressed in terms of a fictitious bottom profile having the form of a parabola coinciding with the actual depth at a point 120 km. from the head of the Gulf. In the previous section the relation of the maximum tidal currents to the amplitude of the tide, the distance from shore and depth was developed. Using equation (9) we can compute the maximum velocity of the tidal currents along the section in the Gulf of Panama. Curve IV in figure 75 represents the computed average amplitude of the tide along this section adjusted to agree with the amplitude at Balboa. Using tidal amplitudes obtained in this way the maximum tidal current velocities were computed for intervals of 10 km. using the actual profile of the bottom. The curve has been extended beyond the shelf by assuming that the tidal amplitude remained constant in the deeper water. The velocities computed in this way are shown in Figure 75, curve V. It can be seen that in deep water the tidal current velocities will be very small, but they increase rapidly over the continental slope and reach maximum values of more than 0.26 m/sec (0.5 knot) near the edge of the continental shelf. The velocities remain high and relatively constant for a considerable distance and then drop off on approaching the head of the Gulf. We might have expected such a velocity distribution as the profile of the bottom in this portion of Gulf is such that the slope is practically constant and equal to $\frac{h}{x}$. As the general form of the bottom profile is parabolic rather than a straight line curve it was considered of interest to compute the velocities that would exist if the bottom was represented by the parabola used in computing the tidal amplitude. This was done and the values are shown in curve VI. In this case the velocities show the maximum at the edge of the shelf, but

decrease rather regularly with the decreasing depth and then drop off sharply near shore.

Relation of tidal currents to range of the tide in the Gulf of Panama.—In the foregoing discussion the maximum velocities along the section have been computed for the average range in tide. As there is such a difference in the neap and spring tidal ranges and as the tidal currents for any tidal period will depend upon the range of the tide, it is necessary to have an expression to relate the velocity distribution to the range of tide. The maximum tidal current velocities at any point along the section in the Gulf of Panama depend upon the integral of the amplitude of the tide between

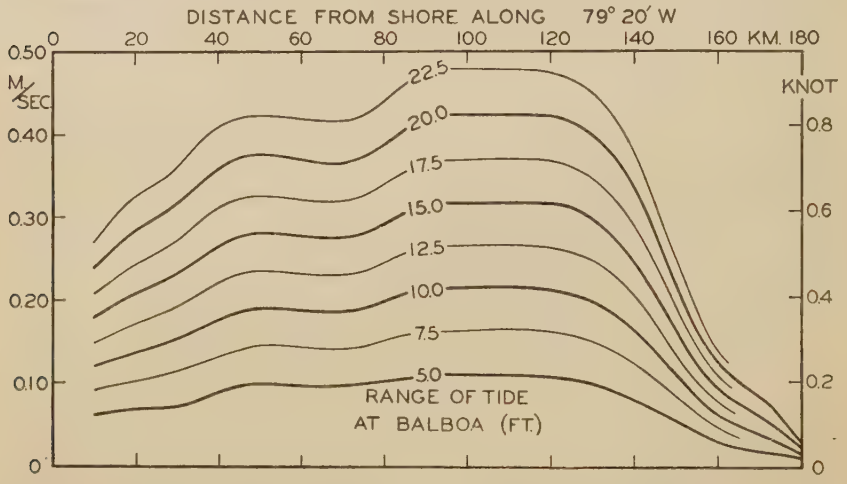

Figure 76. The relation of the maximum tidal current velocities along 79° 20′ W. in the Gulf of Panama to the range of tide at Balboa.

that point and the head of the Gulf. The variations in the range of the tide within the Gulf is rather small compared to the range itself, namely about 19%. Therefore the use of a mean range of tide would not affect the calculation of velocities at any point along the section by more than 10%. From equation (6) we know that the amplitude 120 km for the head of the Gulf, $C = \frac{\eta_o}{1.19}$ when η_o is the range at the head of the Gulf. The mean amplitude on this section is $\bar{\eta} = 1.11\ C$ or $\bar{\eta} = \frac{1.11 \times \eta_o}{1.19} = .934\ \eta_o$. Using the relationship $u_{max} = \frac{x}{h}\sigma \times 0.934\ \eta_o$ the distribution of maximum tidal current velocities along the section was computed for various ranges of tide at Balboa. These are shown in Figure 76.

Relation of tidal current velocities to stage of tide.—In the previous discussion we have considered only the maximum current velocities attained during any tidal cycle and have shown how these vary with the range in tide. As the tidal wave in the Gulf of Panama has the character of a standing wave these maximum velocities are reached at half tide, At high and low water the velocities approach zero. The change in velocity during a tidal cycle follows a simple harmonic form as shown by equation (8). The average velocity of the tidal current for one-half the tidal period, that is between low and high water, or high and low water is $\frac{2}{\pi}$ times the maximum velocity. Using the value of maximum velocities attained at 100 km from

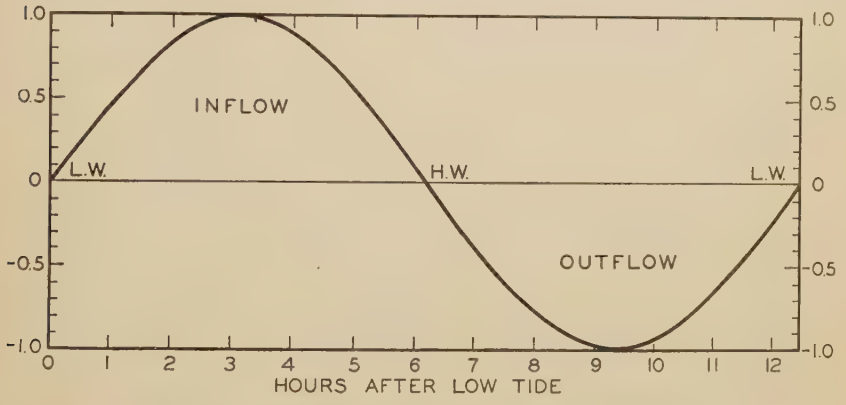

Figure 77. The relation of the velocity of the tidal currents to the phase of the tide in the Gulf of Panama.

the head for mean range of tide, namely 0.26 m/sec, we find an average velocity of 0.17 m/sec which is equivalent to a movement of about 2 nautical miles during the half tidal period. During spring tides the movement will be of the order of 4 nautical miles in each direction.

Figure 77 shows the relation of the tidal current velocity to the phase of the tide. The velocity at any point along the section in the Gulf of Panama and at any phase of the tide and for any range of tide can then be determined from figures 76 and 77 by multiplying the maximum velocity for the necessary range of tide by the fraction appropriate for the phase of the tide. Positive values indicate inward flow, negative values flow out of the Gulf.

Vertical variations in velocity of tidal currents.—In the foregoing discussion it has been assumed that the horizontal velocities were uniform from the surface to the bottom. That is, that particles in a vertical plane normal to the orientation of the wave would remain in such a plane. That such conditions do not hold in nature has been shown whenever careful observations

have been made on the velocity of tidal currents between the surface and bottom (Sverdrup, 1929, for example). Maximum velocities are encountered at or near the surface and below this the velocities decrease towards the bottom. The form of the velocity curve varies considerably but approaches zero at or near the bottom. As our calculations concerning the tidal currents are based on the assumption of uniform horizontal velocities, it is obvious that the values obtained are smaller than those which must exist at and near the surface. The economy of the systems under consideration must be met; that is, a certain amount of water must pass through a given section and if the velocities are small near the bottom, they must be correspondingly greater near the surface.

Vertical components of tidal currents.—In a study of the tidal currents only the horizontal movements are considered as they are of much greater magnitude than the vertical movements. However, it is obvious that some vertical movements must be present, otherwise we could not have the changes in tide level.

Although we are ignoring statements made in the previous section, let us again assume that the horizontal velocities in a vertical plane normal to a standing wave crossing the shelf are constant. If the shelf is of uniform depth, the vertical component will then be zero at the bottom and at the surface equal to the rate of change of tide level. However, if the depth is shoaling, particles near the bottom must rise with the decreasing depths. The magnitude of the vertical change between high and low water will then depend upon the distance travelled by the particle and the slope of the bottom.

Let $\frac{\Delta x}{t}$ = horizontal velocity component, then $\frac{\Delta h}{t}$ = vertical component of velocity.

So that the $\frac{\textit{Vertical velocity}}{\textit{Horizontal velocity}} = \frac{\Delta h/t}{\Delta x/t} = \frac{\Delta h}{\Delta x}$ = slope.

Therefore the vertical velocity at any point on the bottom is determined by the horizontal velocity and slope of the bottom and the vertical range is determined by the horizontal distance travelled during one half tidal period multiplied by the mean slope of the bottom. Using data from Figure 75, the maximum velocities for the average range of tide at points 5, 15, 25, etc. km along the section were read off and the total horizontal movement for rising or falling tides computed. The average slopes at these points were then determined and from these the amount of vertical movement at the bottom. These are shown in Figure 75, curve VII. Along the stretch from the head to entrance of the Gulf the vertical movement near the bottom varies from less than 1 meter to over 50 meters. As the slope of the bottom

at any point is constant and the vertical range is a function of the horizontal movement at that point, the vertical range will depend upon the range of the tide and will, in the Gulf of Panama, vary from less than half the plotted values to nearly twice those shown, depending on the range in tide. It may be seen that, although the distance travelled is relatively small on the continental slope, the slope (Figure 75, curve VIII) is so great that the vertical movement must be great.

Near the edge of any continental shelf and on the continental slope there must be vertical movements of considerable amplitude directly associated with the tidal currents. It should be possible to detect such vertical oscillations by the changes in physical and chemical conditions. These vertical movements will be greatest near the bottom and will decrease towards the surface in direct proportion to the depth of observation to the total depth, if we disregard the convergence or divergence and change in tide level. It should be pointed out that these fluctuations are not the same as internal waves which are encountered in the open ocean.

Tidal currents in the Gulf of Panama.—In the foregoing discussion the variations in the tidal currents in the Gulf of Panama are related to the variations in the range and phase of the tide. The velocity distribution is shown to depend upon the form of the Gulf and the shallow depths which extend a long way out in the Gulf. As the calculations were made on the assumption that the Gulf was of uniform breadth and as the velocity distribution was based on a single profile of the Gulf, it is obvious that the numerical values presented would be modified if the actual shape of the Gulf and the presence of the islands were taken into account. For example, the entrance to the Gulf is narrower than the central portions of the Gulf, and this will cause somewhat higher current velocities at the entrance. The Gulf of San Miguel and its tributary tidal waters will also increase the velocities in the central eastern portion of the Gulf. Around the islands we shall also have tidal currents of higher velocities. The numerical data presented are therefore approximations of the actual conditions arrived at by certain simplifications of the problem.

The tidal currents are independent of any non-tidal movements. During the greater part of the year there is apparently a counter-clockwise gyral within the Gulf which has a velocity of approximately 0.26 m/sec (0.5 knot). The tidal currents must then be superimposed upon this current. The resultant combination of the two will yield the following general result. On the flood tides the northerly movement will be increased in the eastern portion of the Gulf and the southerly movement reduced in the western part of the Gulf. On ebb tides the northerly motion will be reduced in the eastern portion of the Gulf and the southerly movement increased in the western portion. Whether or not the actual movements in any part of the Gulf will be reversed due to the changing tidal currents or will merely be

modified will obviously depend upon the relative strength and direction of the tidal and non-tidal currents.

SUMMARY

1. The tides in the Gulf of Panama and along the Pacific coast of Central America are of the semi-diurnal type associated with a standing wave.

2. The range of tide in the Gulf of Panama varies from 5 feet at neap tides to over 22 feet at springs.

3. The increase in range of tide in the inner part of the Gulf (19%) is shown to be due to the shoaling bottom.

4. A general expression for the effect of the profile of the continental shelf upon the distribution of the velocities of the tidal currents is developed.

5. From the range in tide and the bottom profile of the Gulf of Panama the distribution of current velocities along a section extending out from the head of the Gulf has been computed.

6. The relation of the current velocities to the range and the phase of tide is given.

7. It is pointed out that there should be detectable fluctuations in the vertical distribution of properties near the edge of the continental shelf which are directly associated with the transport of water by the tidal movements.

REFERENCES

1. Harris, R. A.
Manual of Tides. U. S. Coast and Geodetic Survey. Washington.

2. Kirkpatrick, R. Z.
1926. Panama Tides. United States Naval Institute Proceedings, *52*, 4, pp. 660–4.

3. Lamb, Horace
1932. Hydrodynamics, 6th Edition. Cambridge, at the University Press.

4. Sverdrup, H. U.
1929. The Waters on the North Siberian Shelf. Norwegian North Polar Expedition with the "Maud," 1918–1925, Scientific Results, IV, 2. Bergen.

THE RELATION OF DISSOLVED OXYGEN TO NITROGEN IN SOME ATLANTIC WATERS

By

NORRIS W. RAKESTRAW AND VICTOR M. EMMEL

*Woods Hole Oceanographic Institution**

The use of the oxygen content of sea water to indicate the state of biological activity has become such common practice that one is apt to lose sight of the fact that it is subject to certain qualifications. Since it is based on the assumption that the water was originally saturated with oxygen, the momentary temperature and salinity must be observed, and results are often expressed in terms of "percentage saturation," the ratio of the present content of oxygen to that of water of the same temperature and salinity saturated with oxygen from the atmosphere. In this way, values for "percentage saturation" of more than 100% are frequently obtained. The conditions of this supersaturation must be kept in mind, however; the water is frequently under a very considerable pressure, preventing the actual escape of gas, except at the surface.

Assuming the water to have been saturated by contact with the atmosphere, any subsequent change in its temperature or salinity will produce an apparent change in its "percentage saturation." This may be the result of either the warming of the water from above or mixing with water of different temperature and salinity. A study of the solubility data for oxygen, or any of the other atmospheric gases, shows that the mixing of two water-masses at different temperatures, each saturated with gas, results in water with a gas content greater than the saturation content at the intermediate temperature.

On the other hand, the oxygen may actually increase, as the result of photosynthesis. It is also possible to bring about a state of supersaturation, although only to a slight extent, if the surface water is churned up with very small bubbles of air.

These various effects, however, are small compared with the observed differences in oxygen content of the water, so that the usual uncritical use of oxygen data is adequate for most purposes. But in the case of small oxygen differences it is necessary to have some means of evaluating the effects of the various physical factors if the real change in oxygen content is to be calculated exactly.

It is evident that this can be done by observing one of the more inert atmospheric gases, which is subject to the same physical and hydrographic

* Contribution No. 182.

influences as the oxygen, but which is really unchanged by either chemical or biological processes. Nitrogen would seem to be well adapted to this use, since its analytical determination, although more difficult than that of oxygen, is very much easier than that of any of the minor inert gases. Buch (*1*) has done this with some of the oxygen and nitrogen data in the earlier literature and has been able by this means to clear up the relation between assimilation and production of oxygen in some of the more obscure cases.

The increased attention which is now being given to the question of the oxygen minimum layer at deep sea stations, makes it more than ever necessary to be able to distinguish clearly between physical, hydrographic, chemical and biological influences upon the oxygen content.

The analytical determination of nitrogen gas in sea water is not easy, especially if one wishes to separate it from the inert gas fraction (argon, etc.) and not be satisfied simply with the "atmospheric nitrogen" left as residue after removing carbon dioxide and oxygen from dry air. Although this latter step may not be altogether necessary for the purposes described above, we have developed a reasonably simple method of doing so (*3*), primarily for use in some other studies, and have applied it to obtain the pure nitrogen content of water from several deep stations, for comparison with simultaneous oxygen determinations. The original development of such a method for obtaining real nitrogen values, rather than those by difference, was prompted by the feeling that there may very possibly be other inert gases than argon (such as hydrogen, hydrocarbons, etc.) present in some cases. That this was not altogether unwarranted will appear presently.

Buch (*1*) compared the oxygen and nitrogen solubility data from Fox' tables (*2*) and established a relation by which the saturation content of oxygen in water could be readily calculated from the temperature, salinity and nitrogen content. Assuming, then, that the nitrogen in the water has been unaffected by any chemical or biological changes since its original saturation, but that its apparent changes in "percentage saturation" are only the result of temperature and salinity variations in the water, it is possible to calculate a corresponding oxygen content which is the proper base-line from which to measure subsequent changes.

As we have pointed out previously (*4*), our own values for the solubility of pure nitrogen in sea water, as determined by our method, differ significantly from those for "atmospheric nitrogen" in Fox' tables. These revised values are reprinted in Table I. When these data are plotted against oxygen solubility at corresponding temperatures and chlorinities (taken from Fox) a linear relation is obtained between oxygen and nitrogen, which is independent of either temperature or chlorinity, over the range covered. This of course means that over this range the solubilities of both oxygen

and nitrogen are affected similarly by changes in temperature and chlorinity. As shown in Fig. 78, therefore, when the nitrogen content is known the corresponding saturated oxygen content may be calculated from the relation: $cc O_2 = .577 \times cc N_2 - .22$.

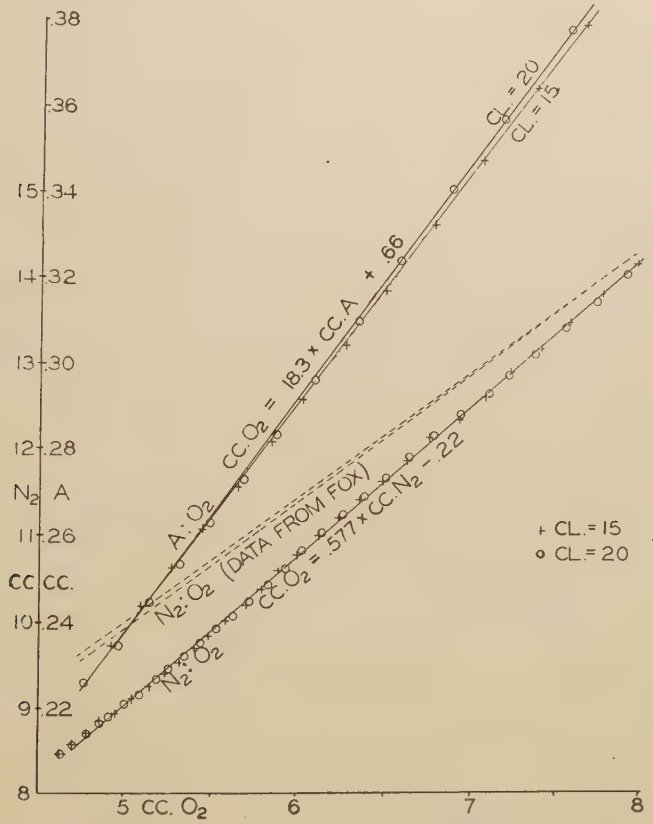

Figure 78. Relation of dissolved oxygen to nitrogen, and to argon, between 0° and 30° C., and chlorinities 15 to 20. Also showing the relation taken from Fox' data for "atmospheric nitrogen" (including argon).

The analytical determination of nitrogen leaves a residue which may also be measured and expressed as argon, although of course it includes any other inert gases as well. From these residual values we have also measured the solubility of crude "argon" in sea water (*4*) and have reprinted the results in Table II. The argon analyses are probably no more accurate than to about 5% under ordinary conditions, which must be kept in mind in the later discussion. However, these data have also been compared with the

solubility of oxygen at corresponding temperatures and chlorinities, and Fig. 78 shows a satisfactory linear relation between the two, but varying somewhat with chlorinity. We have accordingly used the "argon" figures also as a basis for the calculation of oxygen, although the results are more erratic and apparently not so well suited to the purpose as are those for nitrogen.

It must be kept in mind that the use of nitrogen values as a basis for the calculation of oxygen is predicated on the assumption that the nitrogen in the water is not affected by either chemical or biological changes. We are now carrying on a study to determine whether or not this is true, and while there are indications that free nitrogen may, under some conditions, undergo small changes, the regularity of the nitrogen content of deep-sea water and its close approximation to a condition of apparent saturation gives no reason as yet to doubt that it is substantially inert in the sea.

An example of this is found at Station 2899, at which the nitrogen content is almost identical with the saturation content at the temperatures throughout the whole water mass. It is evident that concentration equilibrium has been established along the whole column by diffusion of gas, and it would be exceedingly valuable to have a measure of the rate at which this process takes place.

Table III gives the data from several Atlantic stations, including the nitrogen values, obtained by the method mentioned above, as well as the "residual" figures for crude argon (containing other inert gases). Oxygen was determined by the customary Winkler method, for although the volume of dissolved oxygen is also measured in the course of the nitrogen analysis, these volumes will be lower than the true values, since the samples will have stood for some time.

The interpretation of the various symbols heading the columns in the table is as follows:

D = depth in meters

T = temperature in °C.

Cl = chlorinity pro mille

O_2 = observed oxygen content in ccs. per liter

O_2' = saturation oxygen content at the observed T and Cl (from Fox)

$\%O_2$ = "percentage saturation" of oxygen: $100 \times O_2/O_2'$

N_2 = observed nitrogen content

$\%N_2$ = "percentage saturation" of nitrogen: $100 \times N_2/N_2'$

A = observed content of residual crude "argon"

$\%A$ = "percentage saturation" of crude argon (as for N_2 and O_2)

$O_2{}^N$ = original oxygen content, calculated from the observed N_2, by the relation given in Fig. 78

$O_2{}^A$ = original oxygen content, calculated from A, by the relation given in Fig. 78

Since physical and hydrographic factors affect the oxygen and nitrogen identically, then, if the nitrogen content has not been altered by chemical or biological changes, it should be possible accurately to calculate the original oxygen content from the nitrogen. The relation of the original oxygen to that observed may be expressed in several ways. A comparison of the "percentage saturation" of the two gases may be made. That of the oxygen will correctly indicate the production or assimilation of oxygen if that of nitrogen does not vary from 100%. It may be seen from the tables that such variation is indeed not great, being significant in a few cases only. The customary uncritical use of the "percentage saturation" of oxygen is therefore justified on the whole, particularly in deep water. In all such cases the difference between O_2 and O_2' is a close measure of the real change in oxygen content. On the other hand, $O_2{}^N$, calculated from the nitrogen content, is a more rigorous indication of the original oxygen. The difference between this and the observed oxygen is the corrected, true change in oxygen. Where this difference is positive oxygen has been consumed, where it is negative, as shown here in a few cases, oxygen has been produced in excess of its utilization. And in all such cases, of course, the "percentage saturation" of nitrogen will be greater than that of oxygen.

One of the important outcomes of this method of calculation is the revelation that this predominance of oxygen production over assimilation occurs more rarely than hitherto supposed. This should have some effect upon studies of the relation of photosynthesis to respiration in the sea.

Although similar calculations have been made from the "argon" content it is readily apparent that this function is much less reliable than the nitrogen content. Not only are the figures less accurate but they are erratic for another reason. In the data from Stations 2893 and 2899 the oxygen values calculated from the "argon" are higher than those calculated from the nitrogen in the upper levels, but lower than those calculated from the nitrogen in the deeper samples. It is reasonable to suppose that the "argon" values are somewhat too high in the shallower samples, due to traces of other gases (e.g. hydrogen or hydrocarbons), perhaps the result of the decomposition of plankton, which is present in larger amounts in those samples than the deeper ones.

The figures for the deeper samples at Station 2893 are also somewhat in error, due to another cause. When these samples were analyzed it was noted that small bubbles of air had come out of solution, as the sample-bottles had stood for some time and warmed up. This error, amounting

to nearly 5%, affects the nitrogen and "argon" values, but not the oxygen, since the latter had been obtained immediately by the Winkler method. Later, to avoid this, all the deeper, colder samples were stored under pressure, and at low temperature, until analysis, to prevent the escape of gas.

Figures 79, 80 and 81 have been drawn from the data for Stations 2643, 2899 and 2901 to show the relations between the various functions more graphically. It is believed that the curve for $O_2{}^N - O_2'$ shows the changes in the oxygen content of a water mass most conveniently and accurately.

REFERENCES

1. Buch, K.
   1929. Die verwendung von stickstoff- und sauerstoffanalysen in der meeresforschung. Journal du Conseil, vol. 4, no. 2, pp. 162-191.
2. Fox, C. J. J.
   1907. On the coefficients of absorption of the atmospheric gases, etc. Publications de Circonstance. Con. Perm. Intern. Exp. Mer. no. 41.
3. Rakestraw, N. W. and Emmel, V. M.
   1937. The determination of dissolved nitrogen in sea water. Industrial and Engineering Chem. (Anal. Edit.), vol. 9, p. 344.
4. Rakestraw, N. W. and Emmel, V. M.
   1938. The solubility of nitrogen and argon in sea water. Journal of Physical Chemistry. (In press.)

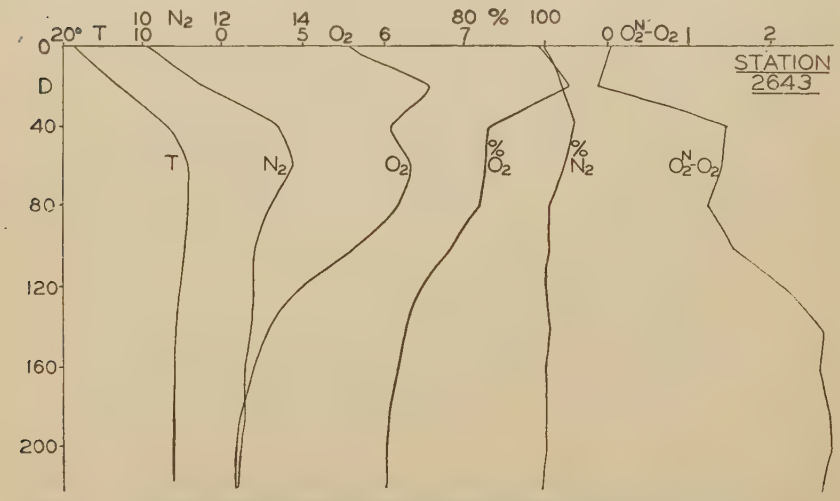

Figure 79. Vertical distributions at Station 2643 of Temperature (T), Nitrogen (N_2), Oxygen (O_2) and the difference between original oxygen contents calculated on the basis of nitrogen present and the observed oxygen contents ($O_2{}^N - O_2$). Nitrogen and Oxygen expressed in absolute values at the left and in per cent relative saturations at the right. Scales for absolute N_2, O_2 and $O_2{}^N - O_2$ in cc. per liter. Depths in meters.

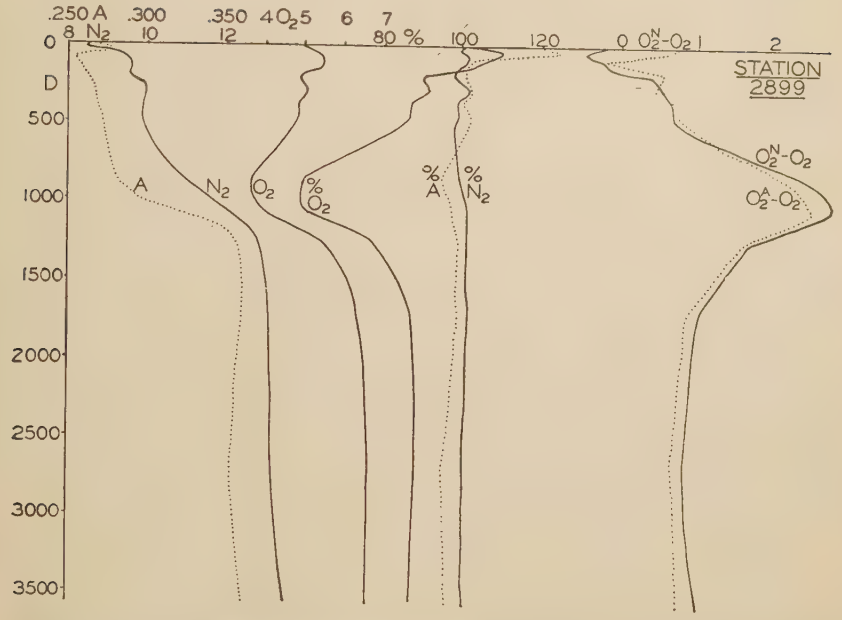

Figure 80. Vertical distributions at Station 2899. (A) Argon. ($O_2^A - O_2$) difference between original oxygen contents calculated on the basis of Argon present and the observed oxygen contents. For further explanations see legend of Figure 79.

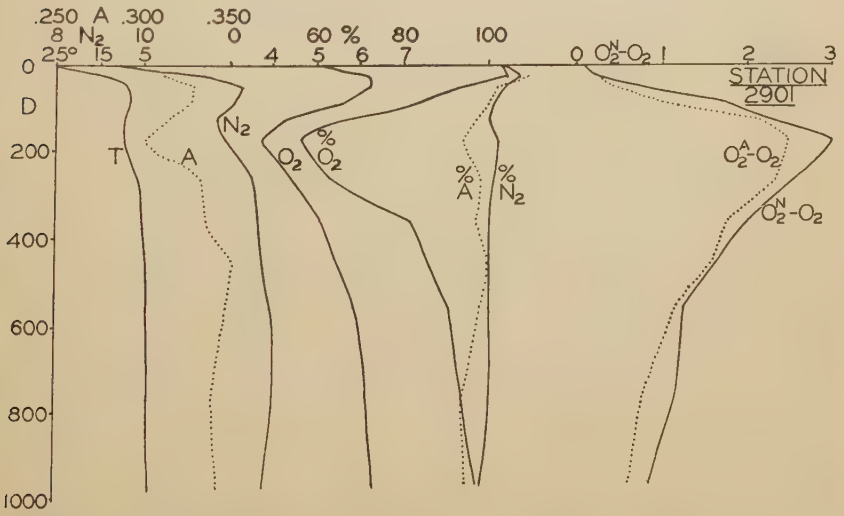

Figure 81. Vertical distributions at Station 2901. See legends of Figures 79 and 80.

TABLE I

Solubility of Nitrogen in Sea Water

(Cc. at S.T.P. per 1000 cc. of Water, from a Normal Atmosphere of 760 mm.)

T	*Cl*	*15*	*16*	*17*	*18*	*19*	*20*	*21*
0°		15.22	15.02	14.82	14.61	14.40	14.21	14.01
1		14.81	14.61	14.42	14.23	14.04	13.85	13.66
2		14.43	14.24	14.06	13.88	13.69	13.51	13.33
3		14.07	13.89	13.72	13.54	13.36	13.19	13.01
4		13.73	13.56	13.40	13.24	13.06	12.89	12.72
5		13.43	13.26	13.10	12.94	12.78	12.62	12.45
6		13.14	12.98	12.82	12.67	12.51	12.35	12.19
7		12.88	12.72	12.56	12.41	12.26	12.10	11.95
8		12.62	12.47	12.32	12.17	12.02	11.87	11.71
9		12.38	12.23	12.08	11.94	11.79	11.64	11.49
10		12.15	12.00	11.86	11.71	11.56	11.42	11.27
11		11.92	11.78	11.63	11.49	11.34	11.20	11.06
12		11.69	11.56	11.42	11.28	11.13	10.99	10.85
13		11.47	11.34	11.21	11.07	10.93	10.79	10.65
14		11.25	11.13	10.99	10.86	10.73	10.59	10.45
15		11.04	10.92	10.79	10.66	10.53	10.39	10.26
16		10.83	10.72	10.59	10.47	10.34	10.21	10.08
17		10.63	10.52	10.40	10.28	10.15	10.03	9.91
18		10.44	10.33	10.21	10.10	9.98	9.86	9.74
19		10.26	10.15	10.03	9.92	9.81	9.69	9.58
20		10.08	9.98	9.87	9.76	9.65	9.54	9.43
21		9.91	9.82	9.71	9.61	9.50	9.39	9.28
22		9.75	9.66	9.56	9.46	9.35	9.24	9.14
23		9.60	9.51	9.41	9.31	9.20	9.10	9.00
24		9.45	9.36	9.26	9.16	9.06	8.96	8.86
25		9.30	9.21	9.11	9.02	8.92	8.82	8.73
26		9.16	9.07	8.97	8.88	8.79	8.69	8.60
27		9.02	8.94	8.84	8.75	8.66	8.56	8.47
28		8.89	8.84	8.72	8.62	8.53	8.44	8.35

TABLE II

Solubility of Argon in Sea Water

(Cc. at S.T.P. per 1000 cc. of Water from a Normal Atmosphere of 760 mm.)

T	*Cl*	*15*	*16*	*17*	*18*	*19*	*20*	*21*
2°		.405	.400	.395	.389	.384	.379	.373
4		.384	.379	.374	.369	.363	.358	.352
6		.365	.360	.355	.350	.345	.340	.335
8		.347	.343	.338	.333	.329	.324	.319
10		.331	.327	.323	.318	.314	.310	.305
12		.317	.313	.309	.304	.300	.296	.292
14		.304	.300	.296	.292	.288	.284	.280
16		.292	.288	.284	.280	.277	.273	.269
18		.282	.278	.274	.270	.267	.263	.259
20		.272	.268	.264	.260	.256	.253	.249
22		.262	.258	.255	.251	.247	.244	.240
24		.253	.249	.246	.242	.238	.235	.231
26		.244	.240	.237	.233	.229	.226	.222
28		.235	.231	.228	.224	.220	.217	.213

TABLE III

D	T	Cl	O_2	O_2'	$\%O_2$	N_2	N_2	A	%A	O_2^N	O_2^A	$O_2^N-O_2$	$O_2^A-O_2$
Station 2643					42°—19′ N; 19°—20′ W					August 10, 1936			
0	18.3	17.6	5.58	5.63	99	10.13	100			5.61		.03	
20	13.0	17.8	6.56	6.17	106	11.50	104			6.42		−.14	
40	6.5	18.1	6.06	7.01	86	13.45	107			7.54		1.48	
60	4.2	18.2	6.32	7.38	85	13.8	105			7.74		1.42	
80	4.2	18.2	6.18	7.38	84	13.22	101			7.42		1.24	
100	4.5	18.4	5.66	7.31	77	12.85	101			7.20		1.54	
120	5.2	18.55	4.97	7.17	69	12.80	100			7.17		2.20	
140	5.7	18.7	4.60	7.08	65	12.76	101			7.26		2.66	
160	5.9	18.75	4.40	7.04	63	12.60	100			7.05		2.65	
180	6.1	18.9	4.24	7.00	61	12.58	100			7.03		2.79	
200	6.1	18.9	4.19	7.00	60	12.50	100			7.00		2.81	
220	6.1	18.9	4.21	7.00	60	12.42	99			6.95		2.74	
Station 2666					39°—00′ N; 70°—00′ W					September 3, 1936			
0	20.90	18.3	5.19	4.98	104	9.72	108			5.38		.19	
10	22.50	18.7	5.04	5.19	97	9.50	102			5.26		.22	
20	11.93	18.6	6.11	6.23	98	11.7	105			6.59		.48	
39	13.34	19.15	4.35	5.92	74	11.0	103			5.93		1.58	
59	12.46	18.85	4.29	6.13	70	11.0	100			6.16		1.87	
78	12.05	19.3				10.8	97						
87	12.31	19.0	4.04	6.16	66	11.1	100			6.18		2.14	
135	7.85	19.1	3.90	6.71	58	11.4	95			6.36		2.46	
183	9.57	19.3	3.20	6.48	49	11.7	101			6.53		3.33	
279	7.71	19.0	4.04	6.75	60	12.4	103			6.93		2.89	
375	5.23	18.9	4.84	7.13	68	12.6	99			7.05		2.21	
471	4.68	19.0	5.19	7.21	72	12.7	99			7.11		1.92	
552	4.69	18.95	5.31	7.21	74	12.5	97			6.99		1.68	
736	4.23	18.9	5.73	7.13	80	12.6	99			7.05		1.32	
921	4.02	19.2	6.02	7.31	82	12.5	96			6.99		0.97	
1105	4.12	19.3	6.08	7.31	83	12.8	98			7.17		1.09	
1381	3.58	19.0	5.90	7.40	80	12.8	97			7.17		1.27	
1845	3.34	18.8	6.21	7.44	84	13.0	98			7.28		1.07	
2762	2.56	19.05	6.24	7.58	82	13.3	98			7.45		1.21	
Station 2667					35°—31′ N; 69°—15′ W					September 5, 1936			
10	26.05	19.8	4.61	4.80	96	8.83	101			4.82		.21	
60	20.91	20.0	5.27	5.22	101	9.67	103			5.36		.09	
180	18.20	19.7	4.72	5.47	86	9.64	98			5.34		.62	
449	17.29	19.5	4.47	5.60	80	10.3	102			5.73		1.26	
719	14.77	19.4	4.10	5.83	70	10.4	101			5.88		1.78	
899	11.54	19.05	3.36	6.20	54	11.3	101			6.30		2.94	
1348	5.18	19.0	5.12	7.13	72	12.6	101			7.05		1.93	
3595	3.14	19.2	6.08	7.47	81	13.9	104			7.88		1.80	

TABLE III (Continued)

Station 2893 35°—30′ N; 67°—17′ W July 12, 1937

D	T	Cl	O_2	O_2'	$\%O_2$	N_2	N_2	A	$\%A$	O_2^N	O_2^A	$O_2^N-O_2$	$O_2^A-O_2$
0	26.5	20.07	4.65	4.73	98	8.8	102	.250	111	4.86	5.23	.21	.58
50	24.0	20.25	5.20	4.93	106	9.3	104	.260	110	5.14	5.41	−.06	.21
100	19.0	20.2	4.97	5.39	92	9.7	100	.270	109	5.38	5.59	.41	.62
150	18.5	20.2	4.86	5.43	90	9.9	101	.280	108	5.49	5.77	.63	.91
200	18.2	20.2	4.80	5.46	88	10.05	102	.290	111	5.58	5.96	.75	1.16
300	17.8	20.2	4.70	5.50	86	10.15	102	.320	120	5.64	6.50	.94	1.80
400	17.5	20.15	4.65	5.53	84	9.9	101	.290	108	5.53	5.95	.88	1.30
500	16.7	20.1	4.40	5.56	79	10.2	101	.295	109	5.66	6.06	1.26	1.66
600	15.5	19.95	4.10	5.74	72	10.4	101	.290	105	5.78	5.96	1.68	1.86
800	11.5	19.57	3.50	6.22	56	11.3	101	.315	104	6.29	6.41	2.79	2.91
1000	7.5	19.42	4.10	6.74	61	12.3	101	.335	101	6.87	6.78	2.77	2.66
1500	4.2	19.37	5.84	7.26	81	12.6	98	.340	96	7.01	6.68	1.17	1.02
2000	3.5	19.35	6.20	7.37	84	12.7	97	.345	94	7.10	6.95	.90	.75
2500	3.3	19.35	6.20	7.41	84	12.75	97	.350	95	7.13	7.04	.93	.84
3000	3.0	19.32	6.10	7.47	82	12.8	96	.350	94	7.16	7.04	1.06	.94
3500	2.8	19.32	6.07	7.51	81	12.9	96	.355	95	7.22	7.13	1.15	1.06
4000	2.5	19.32	6.00	7.56	79	12.95	96	.355	94	7.26	7.13	1.26	1.13
4500	2.3	19.30	5.90	7.60	78	13.0	96	.360	95	7.28	7.22	1.38	1.32
	Station 2899				36°—01′ N; 69°—57′ W				August 8, 1937				
1	27.37	19.99	4.79	4.67	102	8.60	101	.266	121	4.75	5.52	−.04	.73
23	27.06	20.05	5.05	4.70	107	8.52	100	.275	124	4.70	5.69	−.35	.64
46	25.54	20.14	5.28	4.82	110	8.75	101	.274	120	4.83	5.67	−.45	.39
93	20.97	20.21	5.51	5.20	106	9.51	102	.254	103	5.28	5.30	−.23	−.21
139	19.64	20.24	5.45	5.34	102	9.60	100		101	5.32		−.13	
185	18.84	20.20	4.88	5.40	90	9.52	98	.261	101	5.28	5.42	.40	.54
278	18.25	20.20	5.03	5.46	92	9.96	102	.266	102	5.53	5.46	.50	.43
371	17.89	19.43	4.83	5.54	87	9.89	99	.267	100	5.49	5.52	.66	.69
464		20.17	4.81	5.53	87	9.84	99	.271	102	5.46	5.54	.65	.73
556	16.87	20.11	4.61	5.60	82	9.92	98	.272	101	5.51	5.61	.90	1.00
861	12.36	19.70	3.63	6.09	60	10.80	99	.279	94	6.02	5.76	2.39	2.13
1076	7.78	20.19	3.89	6.62	59	11.95	101	.315	97	6.68	6.41	2.79	2.52
1291	4.98	19.37	5.52	7.12	77	12.82	101	.356	99	7.19	7.11	1.67	1.59
1722	3.96	19.36	6.31	7.29	87	13.05	101	.358	99	7.32	7.16	1.01	.85
2690	3.31	19.36	6.57	7.40	88	13.13	100	.353	95	7.36	7.20	.79	.63
3773	2.55	19.36	6.52	7.57	86	13.49	100	.362	96	7.57	7.27	1.05	.75
	Station 2901				39°—40′ N; 71°—43′ W				August 11, 1937				
1	25.05	17.78	5.14	5.01	103	9.43	104			5.23		.09	
25	14.62	18.46	6.18	5.93	104	11.42	107	.314	109	6.38	6.40	.20	.22
50	8.50	19.47	6.25	6.60	95	12.32	104	.329	102	6.89	6.68	.64	.43
87	8.42	18.79	5.59	6.66	84	12.10	101	.326	100	6.76	6.62	1.17	1.03
131	9.49	19.24	4.27	6.48	66	11.70	100	.314	100	6.53	6.40	2.26	2.13
176	9.22	19.38	3.64	6.51	56	11.91	102	.299	94	6.66	6.13	3.02	2.49
268	6.40	19.33	4.40	6.92	63	12.48	101	.332	98	6.98	6.73	2.58	2.33
363	5.40	19.33	5.06	7.07	72	12.62	100	.336	97	7.06	6.80	2.00	1.74
460	4.87	19.34	5.50	7.15	77	12.73	100	.352	100	7.13	7.10	1.63	1.60
560	4.48	19.39	5.87	7.21	81	12.89	100	.348	98	7.21	7.02	1.24	1.15
768	4.22	19.35	6.12	7.26	84	12.96	100	.340	94	7.26	6.87	1.14	.75
977	3.98	19.36	6.32	7.29	87	12.73	98	.343	95	7.13	6.93	.81	.61

SOME ENERGY RELATIONS BETWEEN THE SEA SURFACE AND THE ATMOSPHERE*

By

GEORGE F. McEWEN

Scripps Institution of Oceanography†
University of California
La Jolla, California

ABSTRACT

Interrelations between processes of radiation, convection, and evaporation near the sea surface are determined quantitatively, for the North Pacific Ocean. The object was to investigate these processes of heat changes as a whole rather than to consider any one of them in detail. In particular, revised values of a coefficient giving the time rate of temperature change were determined for use in a method of calculating surface currents from temperature. Observations of a twenty-year series of North Pacific Ocean surface temperatures in an eastern area extending from latitude 20° to 50° were selected so as to be least influenced by ocean currents. Monthly averages for 5° quadrangles prepared and published by the Imperial Japanese Observatory at Kobe were used as a basis for calculating these normal temperatures corresponding to half degree latitude intervals. Values of the average daily solar radiation reaching the sea surface, during each month, prepared and published by H. H. Kimball of the U. S. Weather Bureau and measurements of the amount of solar radiation at various depths provided the additional observational material used. Equating the time rate of change of the amount of heat in an elementary volume of water to that furnished by the absorption of penetrating solar radiation less the rate of loss led to a simple differential equation whose solution expressed the theoretical sea temperature in terms of time, latitude and depth for depths less than 35 meters. The amount of solar radiation at each of a series of depths was assumed to be reduced in a constant ratio for each of the equal depth intervals, and the rate of loss of heat was assumed to vary in proportion to the temperature.

These theoretical temperatures agreed closely with the observed ones. The coefficient in the expression for the rate of loss of heat was calculated first from its relation to the lag (one to three months) between maximum temperatures and maximum radiation, and minimum temperatures and

* Presented at Section of Meteorology of the A. A. A. S. at Denver, June, 1937.

† Contributions from the Scripps Institution of Oceanography. New Series, No. 25.

minimum radiation, and second from the seasonal temperature range and solar radiation observations. Also values of various quantities in the temperature equation based upon observations of solar radiation agreed well with those obtained from the temperature itself.

The amount of radiation penetrating the sea surface was calculated by assuming it to be proportional to that reaching the surface. This required determinations of the absorption coefficient of radiation, values of which were found from the literature on measurements of the radiation at various levels. Values ranging from about .08 up to .45 were listed, the median being about .22.

Since the mean annual amount of heat at any level depends only upon the position, the average rate at which heat is received from the penetrating radiation equals the rate of loss. Therefore, by means of corrections already determined for finding the part of the heat loss due to evaporation, this loss can be expressed in terms of the evaporation expressed in meters per month. This theoretical rate of the mean annual evaporation at a series of latitudes agreed well with values found by Wüst who used a partially empirical method for reducing pan observations of evaporation to evaporation from the sea surface.

FUNDAMENTAL ASSUMPTIONS AND MATHEMATICAL FORMULATION

Essentially the basis is the same as that of an earlier paper (McEwen, 1919) dealing primarily with the oceanic circulation. But an improved procedure is developed, and additional results are deduced. Moreover revised values of the quantities are calculated here from recent observations of normal sea surface temperatures of the North Pacific (Kobe Imperial Marine Observatory, 1935) and from later estimates (Kimball, 1928) of the amount of solar radiation reaching a horizontal surface at sea level.

As before, let Q equal the amount of solar radiation penetrating the sea-surface per unit of time, and assume an exponential law of absorption where b equals the absorption coefficient. Then the amount Qe^{-by} reaches the depth y and the amount absorbed by an element of water, of thickness (Δy) and unit horizontal area, equals $Qe^{-by}\ b\ (\Delta y)$. Represent, empirically as before the complex process of cooling of this element due to evaporation from the surface, back radiation from the water, and mixing, by the simple linear function of the temperature, $k\ (\theta - \theta_1)\ \sigma\ (\Delta y)$ where k and θ_1 may vary with depth but may be regarded as constant within latitude intervals of the order five degrees, and σ equals the specific heat.

Then equate the rate of change of heat in the element of water to the rate of gain less the rate of loss, thus

$$\frac{\partial (\sigma\theta\Delta y)}{\partial t} = Qbe^{-by}(\Delta y) - k\sigma(\theta - \theta_1)(\Delta y) \tag{1}$$

which reduces to the fundamental differential equation

$$\frac{\partial\theta}{\partial t} = \frac{Qb}{\sigma} e^{-by} - k(\theta - \theta_1). \tag{2}$$

Assume the penetrating radiation, Q to be proportional to the incident radiation Q_1, which may be closely represented by the approximate expression

$$Q_1 = K_1 \{[a_1 + f_2(x)] \cos \alpha t + f_3(x) + 1\} \tag{3}$$

where x = (latitude − an assumed reference or base latitude), $f_2(O) = f_3(O) = O$, K_1 and a_1 are constants. Then we may write

$$Q = K \{[a_1 + f_2(x)] \cos \alpha t + f_3(x) + 1\} \tag{4}$$

where the constant $K < K_1$. Equation (2) then becomes

$$\frac{\partial\theta}{\partial t} = \frac{Kb}{\sigma} [(a_1 + f_2(x)) \cos \alpha t + f_3(x) + 1] e^{-by} - k(\theta - \theta_1) \tag{5}$$

whose solution is

$$\theta = \frac{B[a_1 + f_2(x)] e^{-by}}{\sqrt{\alpha^2 + k^2}} \cos(\alpha t - \varepsilon) + \frac{B}{k} e^{-by}[f_3(x) + 1] + \theta_1 \tag{6}$$

where $B = \dfrac{Kb}{\sigma}$, $\tan \varepsilon = \dfrac{\alpha}{k}$, ε/α equals the time lag of temperature behind radiation, and $\alpha = \dfrac{\pi}{6}$ corresponding to the 12 month cycle. According to observations, the latitude gradient $\dfrac{B}{k} e^{-by} f_3'(x)$ is constant for moderate depths, therefore $\dfrac{e^{-by}}{k} = \dfrac{1}{k_1}$ is independent of depth.

If θ_1 is assumed to have the value $-\dfrac{B}{k_1} + \lambda \dfrac{B}{k_1} C^{-by} + \theta_3$ where θ_3 and λ are constants to be determined, the temperature equation becomes

$$\theta = \frac{B[a_1 + f_2(x)] k_1 e^{-by}}{k_1 \sqrt{\alpha^2 + k^2}} \cos(\alpha t - t) + \frac{B}{k_1}[f_3(x) + \lambda e^{-by}] + \theta_3. \tag{6a}$$

In accordance with observations that there is practically no temperature gradient at the time of the minimum temperature, when $\cos(\alpha t - e) = 1$,

$$\frac{B}{k_1} e^{-by} \left\{ \frac{[a_1 + f_2(x)]\, k_1}{\sqrt{\alpha^2 + k^2}} + \lambda \right\} = 0. \tag{6b}$$

Since from Table I, the values of $f_2(x)$, found from radiation observations, range from $-.134$ to $.043$ for latitudes 20° to 50° and $k_1 = .4$ the constant value a_1 corresponding to the base latitude, 35° can be used as an approximation to the variable $[a_1 + f_2(x)]$, and $\lambda = \frac{0.326k_1}{.56} = 582k_1$. If the mean annual temperature, 17°.9 at the base latitude 35° is substituted in equation (6), where $f_3(x)$ and the term involving the time are both zero, the result is

$$17.9 = 34.66\, \lambda e^{-by_1} + \theta_3$$

which reduces to

$$\theta_3 = 17.9 - 20.17k_1\, e^{-by_1} = 17.9 - 20.17k = 13.89,$$

where (see page 225) y_1 equals the depth, of the order three meters, on the exponential curve at which the temperature equals that observed at the surface, and the average value of k equals .199.

CALCULATION OF FUNCTIONS AND PHYSICAL CONSTANTS

Equation (6) is a theoretical expression relating the normal temperature θ, or temperature uninfluenced by the general oceanic circulation, and contains certain fundamental physical magnitudes to be determined.

For this purpose observations of solar radiation incident at the sea surface and of normal sea surface temperatures were used. The functions $f_2(x)$, $f_3(x)$, and their derivatives, and the constants in equation (3) of the incident radiation were calculated, using 35° as the base latitude, as shown in Table I. The mean annual radiation (line 3) and seasonal half amplitude (line 6) corresponding to average cloudiness over a strip of 155° to 180° west longitude (see page 229) Kimball (1928) form the observational basis of these calculations.

Surface temperature data suitable for this purpose have been compiled by the Imperial Marine Observatory at Kobe, Japan (1935). From their basic tabulation by months and five-degree quadrangles of a great number of North-Pacific ocean surface temperatures for the period 1911–1930, Table II of normal temperatures and Table III of normal gradients have been computed by interpolation for latitude intervals of one-half degree to facilitate numerical applications. In order to avoid the effect of circulation so apparent in coastal areas a central strip from 155° to 180° west longitude was selected as approximating to a region of normal temperatures.

Before fitting equation (6) to temperature observations various methods of calculating the important coefficient k appearing in the expression of the

rate of cooling will be considered. Using the time lag of the temperature (p. 219) gives $k = \frac{.5235}{\tan (\Sigma - .2)\, 30^\circ}$ where Σ equals the lag in months from June or December 15, and $(\Sigma - .2)$ equals the lag from June or December 21, the times of maximum and minimum solar radiation. Values of k corresponding to the lag are entered in Table IV. The times of maximum temperature and of minimum temperature for a series of latitudes were determined from Table II, and the corresponding values of k are entered in columns (1) and (2) of Table V.

The half annual temperature range and solar radiation can also be used for calculating k as follows: The temperature should, according to equation (6), decrease exponentially from the surface down to moderate depths of the order 50 meters. Actually vertical mixing near the surface due to waves and other disturbances tend to reduce the gradient near the surface. Accordingly the temperature observed at the surface generally corresponds to that on the exponential curve at a small depth of the order three meters below the surface. Using this depth y_1, in the theoretical temperature equation (6), the half annual range of the observed surface temperature has the value

$$\theta_r^1 = \frac{B}{k_1} \frac{[a_1 + f_2(x)]\, k}{\sqrt{\alpha^2 + k^2}}. \tag{7}$$

The gradient of the mean annual surface temperature is

$$\overline{G}_\theta = \frac{B}{k_1} f_3^1(x). \tag{8}$$

Dividing (7) by (8) gives the equation

$$\frac{k}{\sqrt{\alpha^2 + k^2}} = \frac{\theta_r^1}{\overline{G}_\theta} \left(\frac{f_3^1(x)}{a_1 + f_2(x)} \right) \tag{9}$$

whose second member denoted by W can be calculated from Tables II and III and the last line of Table I.

From the relation

$$\frac{k}{\sqrt{\alpha^2 + k^2}} = W \text{ or } k = \frac{\alpha W}{\sqrt{1 - W^2}} \tag{10}$$

where $\alpha = \pi/6$, providing a second method of calculating k, the values in column (3) of Table V were obtained. Values of the half range θ_r^1 found from Table II are entered in column (6) of Table V. The final adjusted values of k based upon the three estimates presented in columns (1), (2), and (3) are entered in column (4), and the corresponding time lags in months from June or Dec. 15 read from Table IV are entered in column 4a.

Values of the coefficient $\frac{B}{k_1}$ can be calculated in three different ways, as follows:

Solving equation (7) for $\frac{B}{k_1}$ gives

$$\frac{B}{k_1} = \frac{\theta'_r \sqrt{\alpha^2 + k^2}}{-[a_1 + f_2(x)]\, k} \tag{11}$$

where, because of the small range of values of k, the constant value .56 may be used for $\sqrt{\alpha^2 + k^2}$. The resulting values of $\frac{B}{k_1}$ are entered in line 6 of Table VI.

From equation (6) the latitude gradient of the mean annual temperature equals

$$\frac{B}{k} e^{-by} f_3^1(x) = \overline{G}_\theta = \frac{B}{k_1} f_3^1(x) \tag{12}$$

or

$$\frac{B}{k_1} = \frac{\overline{G}_{\theta_n}}{f_3^1(x)}$$

which values are entered in line 10 of Table VI.

Again let $\bar{\theta}$ equal the value of the mean annual temperature at the base latitude 35°. Then from equation (6),

$$\theta - \bar{\theta} = \frac{B}{k_1} f_3(x) \text{ or } \frac{B}{k_1} = \frac{\theta - \bar{\theta}}{f_3(x)} \tag{13}$$

whose values are tabulated in line 13 of Table VI. The average values in the last line show a moderate and irregular variation with respect to latitude. Accordingly, they may be replaced approximately by their average $B/k_1 = 34.66$.

Using the value $-.326$ found for a_1 (see Table I) from radiation observations, the value of $[-.326 + f_2(x)]$ can be calculated from the half temperature range as follows. Rearrange equation (7) and substitute the numerical values already found for a_1, $\frac{B}{k_1}$ and $\sqrt{\alpha^2 + k^2}$. The result is

$$a_1 + f_2(x) = \frac{\theta_r^1 \sqrt{\alpha^2 + k^2}}{B/k_1} = [.326 + f_2(x)] = .01615 \frac{\theta'_r}{k}. \tag{14}$$

The values thus calculated and entered in line 6 of Table VII are seen to agree roughly with those found from radiation (see Table I entered in line 7 for comparison. The agreement is much better for the central latitudes 25° to 45° than for the extreme latitudes.

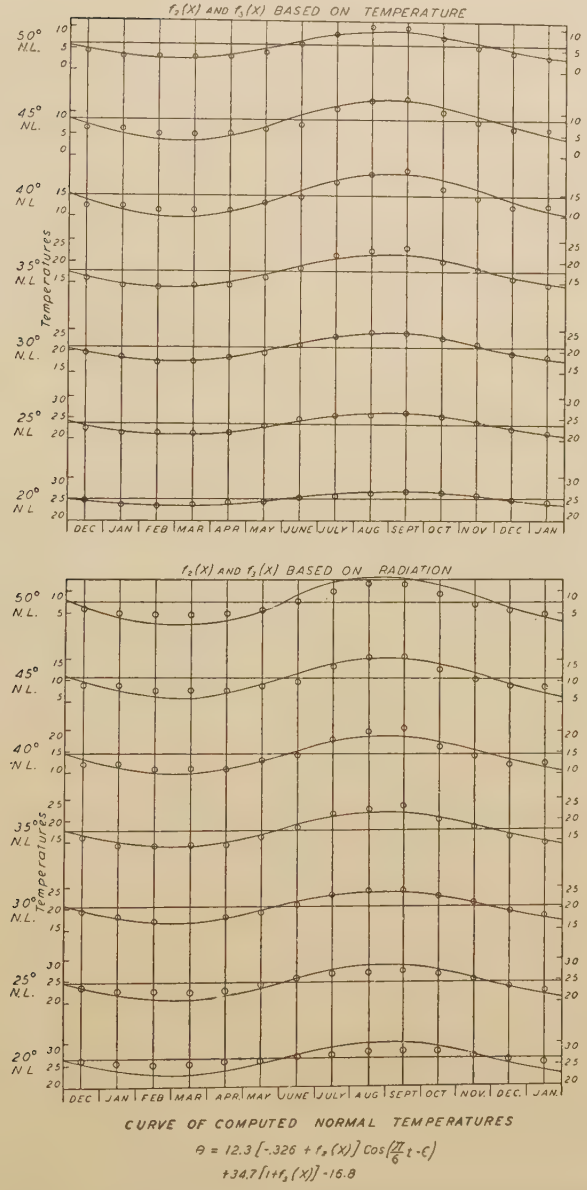

Figure 82. Curves of computed normal temperatures for every 5° northern latitude. See text.

Transforming equation (13) gives the equation

$$f_3(x) = \frac{\theta - \bar{\theta}}{B/k_1} \tag{15}$$

for $f_3(x)$ whose values are entered in line 10 of Table VII. One plus the above values entered in line 11 are seen to agree well with $1 + f_3(x)$ computed from radiation (see Table I) and entered in the last line.

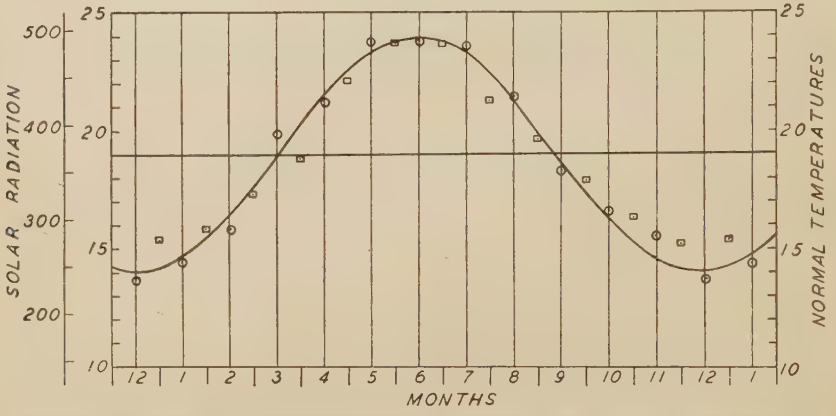

Figure 83. Averages of nine year series (ending December, 1936) of daily solar radiation ⊙ for each month (gram calories per square cm. of horizontal surface) at La Jolla, Lat. 32° 52′ N. and fitted sine curve ——. Normal sea surface temperature ⊡ at the same latitude plotted to a time scale advanced two and one-half months.

Rewrite equation (6) in the form

$$\theta = \frac{B}{k_1}\frac{[a_1 + f_2(x)]\,k}{\sqrt{\alpha^2 + k^2}}\cos(\pi/6\,t - \varepsilon) + \frac{B}{k_1}[\lambda e^{-by} + f(x)] + \theta_3 \tag{16}$$

where

$$\frac{B}{k_1}\lambda e^{-by_1} + \theta_3 = 17.9,$$

the mean annual temperature at the base latitude 35°. Substituting values of the coefficients already determined and values of $f_2(x)$ and $f_3(x)$ calculated from temperature and from radiation, two sets of theoretical values of the temperature can be calculated from equation (16).

Graphs of the theoretical values (Fig. 82) corresponding to $f_2(x)$ and $f_3(x)$, determined from radiation observations are seen to agree well with the observed values indicated by the points. A still better agreement is indicated by the other curves corresponding to $f_2(x)$ and $f_3(x)$ determined from temperature observations. An additional check on the form of the expression used for solar radiation and the corresponding theoretical

temperature equation is indicated by Figure 83 in which the scales of temperature and radiation are so selected that points representing temperature should coincide with those representing radiation if allowance is made for the time lag, about two and one half months. The expression for incident radiation fitted to a nine-year series (Table VIII) of observations at the Scripps Institution, La Jolla is

$$372.2 - 124 \cos. \left(2\pi \frac{t}{12}\right) \tag{17}$$

where $t = 1$ for January. Its graph agrees well with the observed radiation ● and the normal temperature ■ for the same latitude.

THEORETICAL AMOUNT OF SOLAR RADIATION PENETRATING THE SEA SURFACE, AND OF THE RATE OF EVAPORATION FROM THE SEA

It remains to determine the value of $K = \frac{B\sigma}{b}$ of equation (4), where $\sigma = 1$, in order to calculate the amount of solar radiation penetrating the sea surface, or amount actually absorbed by the water. From page 222, $B = 34.66\ k_1 = 34.66\ k\ e^{by_1}$ where y_1 equals the depth on the exponential curve at which, on the average, the temperature equals that observed at the surface.

The theoretical relation of temperature to depth y given by equation (6a) reduces for a given position and time to

$$\theta = M\ e^{-by} + N \tag{18}$$

where M, N, and b are constants. However, vertical mixing near the surface due to waves and other disturbances tends to reduce the gradient. In general observations indicate a practically homogeneous upper layer of the order six meters. Accordingly surface observations correspond to temperatures on the theoretical temperature-depth curve at about half this depth, or roughly three meters.

The absorption coefficient b can be determined from the numerous observations of the amount of the solar radiation at series of depths in the ocean. Typical results, Young and Gordon (1938), presented in table 9 indicate a high variability of b from about .05 to .40, where one meter is the unit of depth. Such a variation is accounted for by the varying turbidity due to varying amounts of material, i.e., silt or plankton in suspension. The average value of k for the latitude interval 20° to 50° is .199. In order to complete the calculation of K a set of units consistent with those used in the tabulation of the incident solar radiation will be used. The incident solar

radiation is the daily amount averaged over a period of one month and expressed in gram calories per day reaching a horizontal surface of one square centimeter. Since in the fundamental equation (1) and those derived from it the unit of time used was one month and the unit of length was one meter the value of $K = \frac{B\sigma}{b} = \frac{B}{k_1}\frac{k\, e^{by_1}}{b}$, which is a time rate, must be divided by 30 to correspond to one day, and the value of b must be divided by 100 to correspond to centimeters. Therefore $K = \frac{B}{k_1}\left(\frac{k\, e^{by_1}}{b}\right)\frac{100}{30} = 34.66 \times .199 \times \frac{100}{30}\left(\frac{e^{by_1}}{b}\right) = 23\left(\frac{e^{by_1}}{b}\right)$ in gram calories per day on a horizontal area of one square centimeter just below the sea surface, or penetrating the sea surface at the base latitude 35°.

The coefficient $\left(\frac{e^{by_1}}{b}\right)$ depends upon the choice of y_1 which is somewhat indefinite and must be averaged over the wide range of values of b. To avoid extreme values the medians of the eight columns of Table IX may be used, and are in their order of magnitude

$$.08, .12, .16, .16, 17, .205, .27, .35.$$

The corresponding values of $\left(\frac{e^{by_1}}{(b)}\right)$ were calculated for

$$y_1 = 3.5, 4.0, 4.5 \text{ and } 5.0.$$

The median values are respectively 10.80, 11.70, 12.81, and 14.01.

The product of this coefficient by 23 must be less than 304, the incident radiation at the base latitude. Also it is desirable to have as small a range or variability as possible in the values of the coefficient with respect to b in order that they may be replaced by a constant value with the least error. The first criterion rules out the largest factor 14.01 corresponding to the depth 5. The least variable values of the remaining three correspond to the depth 4.5 the range being from 12.2 to 17.9. Accordingly, using the corresponding median value 12.81,

$$K = 12.81 \times 23 = 295.$$

Amounts of the penetrating radiation R_p calculated for a series of latitudes using values of $[1 + f_3(x)]$ obtained from temperatures are entered in line 3 of Table X. Amounts of observed incident radiation, R_s are entered in line 14 for comparison. As shown in the last line, the amount of penetrating radiation varies from 88% to 98% of the available incident radiation, corresponding to a loss of 2% to 12% by reflection, which is consistent with accepted values.

Corresponding to a constant mean annual temperature at any latitude, the rate of loss of heat from a surface layer of water must equal that supplied by the penetrating solar radiation. Since this rate of heat loss is due to evaporation, back radiation, and the diffusion of sensible heat into the air, corrections must be applied to obtain the rate of evaporation. The back radiation B_r may be computed by means of equation (8), Richardson (1931), which is an adaptation of the Stefan-Boltzman law of radiation from water to and air. His equation reduces to

$$B_r = 1077.6\ (10^{-5}\ \theta_w{}^4) - 939.6\ (10^{-5}\ \theta_A{}^4)$$

gram calories per day on a square centimeter, where θ_w is the absolute temperature of the water and θ_A is the absolute temperature of the air near the water surface.

The function $(10^{-5}\ \theta^4)$ of the absolute temperature is closely approximated by the following more convenient function of the centigrade temperature θ_c

$$(10^{-5}\ \theta_{abs.}{}^4) = .5555 + .008095\ \theta_c + .0000495\ \theta_c{}^2$$

for θ_c between 0 and 40°. Neglecting the small difference between the air and sea surface temperature the value of the back radiation reduces to

$$B_r = 76.66 + 1.117\ \theta_c + .006831\ \theta_c{}^2.$$

Values of B_r corresponding to the mean annual sea surface temperature entered in line 4 of table 10 are subtracted from those of R_p, line 3. The loss of heat thus corrected for back radiation, expressed in terms of evaporation E_c in meters per month (Table X, line 6) is

$$E_c = \frac{30}{580 \times 100}\ (R_p - B_r) = .000517\ (R_p - B_r)$$

where 580 equals the latent heat of vaporization. The effect of diffusion may be eliminated by means of R, the Bowen's ratio, Bowen (1926), McEwen (1930), which has been found to be about .2 for the ocean, Richardson (1930) page 1006. Therefore, dividing E_c by $1 + R = 1.2$ gives the theoretical evaporation rate (Table X, line 7). Corresponding evaporation rates based upon various methods of correcting observations of evaporating pans, presented in the next three lines, 8, 9, and 10, Wüst (1920, 1936) and Cherubin (1931), agree well with these theoretical values. This agreement is even better than might be expected because of simplifying assumptions made, and the necessarily crude data used in calculating the evaporation rate. Theoretical values of the evaporation rate, Sverdrup (1937), based upon serial values of the relative humidity and atmospheric turbulence confirmed Wüst's later results at the few stations where the data needed were available.

The general agreement of these different methods further supports the validity of this comprehensive procedure for investigating the various

inter-related processes of heat exchange and transformations near the sea surface.

REFERENCES CITED

1. Bowen, I. S.
1926. The ratio of heat losses by conduction and by evaporation from any water surface. Physical Review, 27: 779–787, 1 fig. in text.

2. Cherubim, R.
1931. Über Verdunstungsmessung auf See. Ann. der Hydro. u. Marit. Meteor. 59, Heft 9, pp. 325–334.

3. Kimball, Herbert H.
1929. Amount of solar radiation that reaches the surface of the earth on the land and on the sea, and methods by which it is measured. Monthly Weather Review, Washington, D. C., 56, pp. 393–399.

4. McEwen, George F.
1919. Ocean temperatures, their relation to solar radiation and oceanic circulation. Quantitative comparisons of certain empirical results with those deduced by principles and methods of mathematical physics. Misc. Studies in Agr. and Biol. In Semi-centennial Publ. Univ. of Calif., 1868–1918, pp. 335–421.

5. McEwen, George F.
1930. Results of Evaporation Studies conducted at the Scripps Institution of Oceanography and the California Institute of Technology. Bull. of the Scripps Inst. of Oceanog., Technical Series, Vol. 2, No. 11, pp. 401–415. Univ. of Calif. Press, Berkeley, Calif. 1930.

6. Okada, T.
1935. The mean atmospheric pressure, cloudiness, air temperature and sea surface temperature of the North Pacif. Ocean and the Neighbouring seas during the years 1911 to 1930. The Imperial Marine Observatory, Kobe, Japan.

7. Richardson, Burt
1930. Evaporation as a function of isolation. Proceedings of the American Society of Civil Engineers, 56: 945–960. Also in Trans. of Am. Soc. C. E. Vol. 95 (1931), pp. 996–1019 with its discussion.

8. Sverdrup, H. U.
1937. On the evaporation from the oceans. Sears Found. Journ. Mar. Res. Vol. 1, No. 1, New Haven, pp. 3–14.

9. Wüst, G.
1920. Die Verdunstung auf dem Meere. Veröff des Inst. für Meereskunde an der Universität Berlin. N. F. A., Heft 6, pp. 1–95.

10. Wüst, G.
1937. Oberflächensalzgehalt, Verdunstung und Nieder-Schlag auf dem Weltmeere. Assoc. Oceanog. Phys., Procès-Verbaun No. 2, pp. 79–83.

11. Young, R. T. and Gordon, Robert D.
1938. Report on the Penetration of Light in the Pacific Ocean off the Coast of Southern California. Scripps Institution of Oceanography, Bulletin, technical series (in press).

TABLE I

CALCULATION FROM SOLAR RADIATION OBSERVATIONS OF THEIR RELATION TO LATITUDE AND OF THE GRADIENT OF THESE LATITUDE FUNCTIONS

LATITUDE	*BASE*												
	20	*22.5*	*25*	*27.5*	*30*	*32.5*	*35*	*37.5*	*40*	*42.5*	*45*	*47.5*	*50*
Lat. $-35 = x$ =	−15	−12.5	−10	−7.5	−5	−2.5	0	2.5	5	7.5	10	12.5	15
$K_1[1 + f_3(x)]$ =	379	373	363	345	326	312	$304 = K_1$	290	274	260	241	226	216
$K_1[1 + f_3(x)]/K_1 = 1 + f_3(x)$ =	1.246	1.227	1.194	1.135	1.072	1.026	1.000	0.954	0.901	0.875	0.793	0.743	0.710
$f_3(x)$ =	.246	.227	.194	.135	.072	.026	0.00	− .046	− .099	− .125	− .207	−0.257	−0.290
$K_1[a_1 + f_2(x)]$ =	− 94	−101	−103	− 95	− 90	− 86	− 99	−104	−113	−117	−121	−130	−140
$K_1[a_1 + f_2(x)]/K_1 = [a_1 + f_2(x)]$ =	− .309	− .332	− .339	− .313	− .296	− .283	− .326	− .342	− .372	− .385	− .398	− .458	− .460
$f_2(x)$	.017	− .006	− .013	.013	.030	.043	0.0	− .016	− .046	− .059	− .072	− .102	− .134
$G_R = K_1 f_3{}^1(x)$	−1.1	−3.2	−5.6	−7.4	−6.6	−4.4	−4.4	−6.0	−6.0	−6.6	−6.8	−5.0	−4.8
$f_3{}^1(x)$ =	− .00362	− .01053	− .01841	− .02435	− .02170	− .01448	− .01448	− .01975	− .01975	− .0217	− .02239	− .01645	− .01580
$f_2{}^1(x)$ =		.00585	.00396	.00865	.00596	− .0060	− .0119	− .0092	− .0085	− .0052	− .0086	− .0126	− .0119
$f_3{}^1(x)/f_2{}^1(x)$ =		−1.800	−4.65	−2.79	−3.64	2.41	1.216	2.15	2.33	4.17	2.61	1.306	1.329
$f_3{}^1(x)/[a_1 + f_2(x)]$ =	.0117	.0317	.0543	.0779	.0732	.0512	.0444	.0577	.0531	.0564	.0562	.0384	.0343

TABLE II

NORMAL SEA SURFACE TEMPERATURES OF THE NORTH PACIFIC OCEAN BASED UPON OBSERVATIONS

From 1911 to 1930 Between Longitudes 155°–180° West

Latitude	*Jan.*	*Feb.*	*March*	*April*	*May*	*June*	*July*	*August*	*Sept.*	*Oct.*	*Nov.*	*Dec.*	*Annual Mean*
52.5	3.31	2.90	2.87	3.22	4.35	6.36	8.69	10.28	9.81	7.69	5.71	4.15	5.77
50	3.49	3.11	3.18	3.44	4.44	6.36	8.90	10.56	10.12	8.04	5.92	4.41	6.00
47.5	4.03	3.68	4.03	4.08	4.75	6.72	9.55	11.26	10.97	8.87	6.47	5.05	6.62
45	6.55	5.45	5.40	5.72	6.59	7.82	11.23	13.28	13.50	10.70	8.13	6.94	8.44
42.5	10.94	8.30	7.28	8.28	9.69	9.38	13.79	16.50	17.61	13.46	10.74	9.99	11.32
40	11.83	10.56	10.50	10.61	12.22	13.51	17.27	19.03	20.29	15.96	13.54	11.74	13.92
37.5	12.42	12.62	13.58	12.85	14.53	17.50	20.46	21.24	22.32	18.30	16.29	13.50	16.30
35	14.55	14.11	14.77	14.61	16.18	18.49	21.64	22.81	23.24	20.08	18.34	16.02	17.90
32.5	16.92	15.58	15.64	16.29	17.70	19.05	22.32	23.97	23.82	21.65	20.09	18.45	19.29
30	18.72	17.68	17.45	18.25	19.69	21.41	23.69	24.87	24.87	23.39	21.77	19.84	20.97
27.5	20.28	19.77	19.40	20.15	21.57	23.74	24.92	25.49	25.80	24.88	23.19	21.16	22.53
25	21.64	21.51	21.20	21.82	23.06	24.82	25.51	25.87	26.27	25.77	24.23	22.48	23.68
22.5	22.85	22.59	22.58	23.08	23.86	25.06	25.63	26.00	26.39	26.17	24.93	23.78	24.41
20	23.95	23.29	23.68	24.08	24.26	25.20	25.73	26.10	26.49	26.40	25.48	24.80	24.95

TABLE III

GRADIENTS IN DEGREES CENTIGRADE PER DEGREE OF LATITUDE OF NORMAL SEA SURFACE TEMPERATURES

From 1911 to 1930 of the North Pacific Ocean

Based upon Observations Between Longitudes 155°–180° West

Latitude	*Jan.*	*Feb.*	*March*	*April*	*May*	*June*	*July*	*August*	*Sept.*	*Oct.*	*Nov.*	*Dec.*	*Annual Mean*
52.5	−.01	−.02	−.03	−.02	−.01	−.01	−.01	−.03	−.03	−.05	−.01	−.04	−.022
50	−.14	−.16	−.22	−.17	−.07	−.09	−.17	−.20	−.22	−.24	−.16	−.18	−.168
47.5	−.50	−.40	−.45	−.42	−.40	−.28	−.45	−.47	−.60	−.48	−.40	−.45	−.442
45	−1.38	−.92	−.65	−.84	−.99	−.64	−.85	−1.05	−1.33	−.92	−.86	−.99	−.952
42.5	−1.28	−1.12	−1.03	−1.05	−1.24	−1.11	−1.26	−1.26	−1.53	−1.13	−1.15	−1.07	−1.187
40	−.23	−.88	−1.32	−.92	−.98	−1.72	−1.39	−.96	−.95	−.99	−1.13	−.68	−1.011
37.5	−.52	−.70	−.86	−.80	−.78	−1.00	−.88	−.76	−.58	−.83	−.97	−.86	−.795
35	−.93	−.57	−.36	−.68	−.61	−.24	−.33	−.54	−.27	−.66	−.75	−1.02	−.580
32.5	−.85	−.72	−.52	−.73	−.70	−.58	−.40	−.41	−.32	−.67	−.69	−.78	−.614
30	−.67	−.86	−.77	−.78	−.79	−.99	−.54	−.30	−.41	−.66	−.63	−.53	−.660
27.5	−.59	−.79	−.77	−.73	−.69	−.70	−.37	−.20	−.29	−.49	−.50	−.53	−.554
25	−.51	−.58	−.65	−.60	−.48	−.23	−.11	−.10	−.10	−.27	−.36	−.52	−.376
22.5	−.45	−.29	−.45	−.41	−.17	−.06	−.04	−.03	−.04	−.11	−.22	−.50	−.231
20	−.43	−.27	−.43	−.39	−.15	−.05	−.03	−.03	−.03	−.07	−.21	−.38	−.203

TABLE IV

$$k = \frac{.5235}{\tan[(\Sigma - 2)30°]}$$

Σ Lag from June or Dec. 15	.00	.01	.02	.03	.04	.05	.06	.07	.08	.09	$(\Sigma - .2)$ Lag from June or Dec. 21
1.0	1.176	1.159	1.143	1.128	1.112	1.097	1.083	1.068	1.054	1.041	.8
1.1	1.028	1.014	1.001	.989	.976	.964	.952	.941	.929	.918	.9
1.2	.907	.896	.885	.875	.864	.854	.844	.834	.825	.816	1.0
1.3	.809	.797	.788	.779	.770	.762	.753	.745	.736	.729	1.1
1.4	.720	.712	.705	.697	.689	.682	.675	.667	.661	.653	1.2
1.5	.646	.640	.633	.626	.619	.613	.606	.600	.594	.587	1.3
1.6	.582	.575	.569	.563	.557	.552	.546	.540	.534	.529	1.4
1.7	.523	.518	.513	.507	.502	.497	.492	.486	.481	.476	1.5
1.8	.471	.466	.462	.456	.452	.447	.442	.438	.433	.428	1.6
1.9	.424	.419	.415	.410	.406	.402	.397	.393	.389	.385	1.7
2.0	.380	.376	.372	.368	.364	.360	.356	.352	.348	.344	1.8
2.1	.340	.336	.332	.328	.325	.321	.317	.313	.309	.306	1.9
2.2	.302	.298	.295	.292	.288	.284	.281	.277	.274	.270	2.0
2.3	.266	.263	.260	.257	.253	.250	.247	.243	.240	.236	2.1
2.4	.233	.230	.227	.223	.220	.217	.214	.210	.207	.204	2.2
2.5	.201	.198	.195	.192	.188	.185	.182	.179	.176	.173	2.3
2.6	.170	.167	.164	.161	.158	.155	.152	.149	.146	.143	2.4
2.7	.140	.137	.134	.131	.129	.126	.123	.120	.117	.114	2.5
2.8	.111	.108	.106	.103	.100	.097	.094	.091	.088	.086	2.6
2.9	.083	.080	.077	.074	.072	.069	.066	.063	.061	.057	2.7
3.0	.055	.052	.049	.046	.044	.041	.038	.035	.033	.030	2.8
3.1	.027	.025	.022	.019	.016	.014	.011	.008	.005	.003	2.9
3.2	.000	−.003	−.005	−.008	−.001	−.014	−.016	−.019	−.022	−.025	3.0

TABLE V

Tabulation of the Temperature Factor k, and the Temperature Range and Half Range

Column (1) Values of k calculated from the lag of minimum temp.

(2) Values of k calculated from the lag of maximum temp.

(3) Values of k calculated from temperature range and solar radiation.

(4) Adjusted value of k based upon columns (1) (2) and (3).

(4a) Time lag in months from June or December 21 corresponding to values of k entered in column (4).

(5) Temperature range.

(6) Half range of temperature.

Except for column (3) moving averages of groups of 7 were used.

Values in column (3) and (4) were interpolated within the two and one-half degree intervals,—52.5 to 50, 50 to 47.5 etc.

Latitude	*(1)*	*(2)*	*(3)*	*(4)*	*[4(a)]*	*(5)*	*(6)*
52.5	.192	.265		.228	2.22	7.64	3.82
50	.202	.253		.227	2.22	7.59	3.80
47.5	.203	.235	.185	.209	2.27	7.69	3.85
45	.101	.211	.133	.172	2.39	8.33	4.17
42.5	.031	.211	.135	.173	2.39	10.12	5.06
40	.129	.214	.131	.172	2.39	9.23	4.62
37.5	.404	.255	.175	.215	2.26	8.74	4.37
35	.297	.248	.186	.217	2.25	8.76	4.38
32.5	.159	.221	.196	.208	2.28	8.42	4.21
30	.153	.210	.241	.225	2.23	7.55	3.77
27.5	.179	.199	.263	.231	2.21	6.38	3.19
25	.222	.158	.199	.193	2.33	4.93	2.46
22.5	.238	.155	144	.179	2.37	3.86	1.93
20	.233	.135	.048	.184	2.35	3.19	1.59

TABLE VI

CALCULATION OF THE COEFFICIENT B/k_1 FROM THE ADOPTED VALUE OF k AND FUNCTIONS REPRESENTING THE RELATION TO LATITUDE OF NORMAL SEA SURFACE TEMPERATURES AND SOLAR RADIATION

LATITUDE	*BASE*												
	20	*22.5*	*25*	*27.5*	*30*	*32.5*	*35*	*37.5*	*40*	*42.5*	*45*	*47.5*	*50*
Lat. $-35 = x$ =	−15	−12.5	−10	−7.5	−5	−2.5	0	2.5	5	7.5	10	12.5	15
Half range, θ_r =	1.59	1.93	2.46	3.19	3.77	4.21	4.38	4.37	4.62	5.06	4.17	3.85	3.80
$a_1+f_2(x)$ from radiation =	− .309	− .332	− .339	− .313	− .296	− .283	− .326	− .342	− .372	− .385	− .398	− .428	− .460
k =	.184	.179	.193	− .231	.225	.208	.217	.215	.172	.173	.172	.209	.227
$\frac{\theta_r(.56)}{-[a_1+f_2(x)]k} = \frac{B}{k_1}$ =	15.67	18.17	21.00	24.7	31.7	40.0	34.7	33.3	40.4	42.6	34.1	24.4	20.40
$-k[a_1+f_2(x)]$ =	.0569	.0595	.0655	.0724	.0666	.0589	.0708	.0735	.0640	.0666	.0685	.0885	.1045
$\overline{G}$ =	− .203	− .231	− .376	− .554	− .660	− .614	− .580	− .795	− 1.011	−1.187	− .952	− .442	− .168
$f_3{}^1(x)$ from radiation =	− .00362	− .01053	− .01841	− .02435	− .02170	− .01448	− .01448	− .01975	− .01975	− .0217	− .02239	− .01645	− .01580
$\overline{G}/f_3{}^1(x) = \frac{B}{k_1}$ =	56.1	21.9	20.4	22.7	30.4	42.4	40.0	40.2	51.2	54.6	42.5	26.9	10.6
$\theta - \underline{\theta}$ =	7.05	6.51	5.78	4.63	3.07	1.39	0.00	−1.60	−3.98	−6.58	−8.46	−11.28	−11.90
$f_3(x)$ from radiation =	.246	.227	.194	.135	.072	.026	.000	− .046	− .099	− .125	− .207	− .257	− .290
$\frac{\theta - \underline{\theta}}{f_3(x)} = \frac{B}{k_1}$ =	28.7	28.7	29.8	34.3	42.6	53.5	—	34.8	40.2	52.6	40.9	43.9	41.0
Averages of the three estimates of $\frac{B}{k_1}$ =	33.5	22.9	23.7	27.2	34.9	45.3	38.2	36 1	43.9	49.9	39.2	31.8	24.0
Final Average $B/k_1 = 34.66$													

TABLE VII

CALCULATION FROM NORMAL TEMPERATURES OF THE RELATION TO LATITUDE OF THE SEASONAL RANGE OF SOLAR RADIATION AND OF THE MEAN ANNUAL SOLAR RADIATION USING THE ADJUSTED VALUE OF k AND THE VALUE $B/k_1 = 34.7$, FROM TABLE VI

LATITUDE	*BASE*												
	20	*22.5*	*25*	*27.5*	*30*	*32.5*	*35*	*37.5*	*40*	*42.5*	*45*	*47.5*	*50*
Lat. $-35 = x =$	−15	−12.5	−10	− 7.5	− 5	− 2.5	0	2.5	5	7.5	10	12.5	15
$-\theta_r =$	− 1.59	− 1.93	− 2.46	− 3.19	− 3.77	− 4.21	− 4.38	− 4.37	− 4.62	− 5.06	− 4.17	− 3.85	− 3.80
$k =$	.184	.179	.193	.231	.225	.208	.217	.215	.172	.173	.172	.209	.227
$-\theta_r/k =$	− 8.64	−10.78	−12.74	−13.81	−16.75	−20.3	−20.2	−20.3	−26.9	−29.2	−24.2	−18.4	−16.75
$-.326 + f_2(x) = .01615(-\theta_r/k) =$	− .140	− .174	− .206	− .223	− .270	− .328	− .326	− .328	− .434	− .472	− .391	− .297	− .270
$[-.326 + f_2(x)]$*	− .309	− .332	− .339	− .313	− .296	− .283	− .326	− .342	− .372	− .385	− .398	− .428	.460
Mean annual temperature $\bar{\theta}(x)$	24.95	24.41	23.68	22.53	20.97	19.29	17.90	16.30	13.92	11.32	8.44	6.62	6.00
$\bar{\theta}(x) - \bar{\theta}(o)$	7.05	6.51	5.78	4.63	3.07	1.39	0	1.60	− 3.98	− 6.58	− 9.46	−11.28	−11.90
$[\bar{\theta}(x) - \bar{\theta}(o)]/(B/k_1) = f_3(x)$	.203	.188	.166	.133	.088	.040	0	− .046	− .115	− .190	.273	− .325	− .343
$1 + f_3(x) =$	1.203	1.188	1.166	1.133	1.088	1.040	1.000	.954	.885	.810	.727	.675	.657
$[1 + f_3(x)]$*	1.246	1.227	1.194	1.135	1.072	1.026	1.000	.954	.901	.875	.793	.742	.710

* Computed from radiation.

TABLE VIII

AVERAGE DAILY INSOLATION ON A HORIZONTAL SURFACE, GRAM CALORIES PER SQUARE CENTIMETER, FOR EACH MONTH AT THE SCRIPPS INSTITUTION OF OCEANOGRAPHY

Latitude 32° 52′ N.

( ) Interpolated Values.
[ ] Values supplied from another year assumed to be similar.

Yr.	*Mo.: Jan.*	*Feb.*	*Mar.*	*April*	*May*	*June*	*July*	*Aug.*	*Sept.*	*Oct.*	*Nov.*	*Dec.*	*Summary*	*Average*
1928	[261]	[312]	[395]	(433)	[466]	[449]	(545.1)	(430)	(293)	(296)	(291)	(276.7)	4447.8	370.6
9	(261)	(312.2)	(395.4)	(433)	(467.6)	447.7	437.9	452.5	293.2	296.5	293.5	(270.0)	4360.5	363.4
1930	192.4	259.0	347.8	429.8	454.8	391.3	475.5	395.7	347.6	316.2	255.9	250.3	4116.3	343.0
1	(243.8)	(274.4)	(342)	(385)	372.3	440.6	386.7	333.9	(349.1)	(354.0)	(260.4)	227.0	3969.2	330.8
2	(278.4)	291.9	393.2	469.9	466.7	442.5	414.8	328.1	229.4	234.4	236.7	201.9	3987.9	332.3
3	213.8	292.6	334.8	339.3	411.3	392.2	329.4	459.6	328.4	277.6	322.0	268.2	3969.2	330.8
4	303.4	291.9	382.6	488.9	[605]*	[604]	[533]	[538]	(400)	(346)	[303]	[224]	5019.8	418.3
5	[278.0]	[283]	[403]	513.8†	552.5	519.0	596	478.9	402.0	374.2	289.7	239.8	4929.9	410.8
6	265.1	309.2	412.6	472.7	605.5	604.0	532.9	537.8	450.1	314.9	302.6	224.1	5031.5	419.3
7	263.7	311.7	463.5	529.2	459.2	558.0	(510)	[479]	[402]	[374]	[290]	[240]	4880.3	406.7
Summary	2560.	2938.	3870.	4494.	4861.	4848.	4761.	4433.	3495.	3184.	2845.	2422.	44712.4	
Average	256.1	293.8	387.0	449.4	486.1	484.8	476.1	443.3	349.5	318.4	284.5	242.2		372.6
Formula	264.7	310.2	372.2	434.2	479.7	496.2	479.7	434.2	372.2	310.2	264.7	248.2		

Formula $372.2 - 124 \cos. \left[2\pi \frac{t}{12} \right]$, $t = 1$ for Jan. etc.

* Deterioration of thermo-electric element noted, May 1934.
† New thermo-electric element installed, April 1935.

TABLE IX

VALUES OF THE ABSORPTION COEFFICIENT b FOR SEA WATER, WHERE THE UNIT OF DEPTH IS ONE METER

Determined from Measurements of Radiation

b	*Measurements of Radiation at Plymouth, England*	*Shelford and Gail* — *Measurements of Radiation at Puget Sound*	*Richardson* — *San Diego Region Measurements of Radiation 1931*	*Young* — *San Diego Region 1936*	*Clarke* — *Measurement of Radiation in Coastal Waters of West North Atlantic* — *Violet*	*Blue*	*Green*	*Red*
.00								
1								
2								
3						1		
4				1				
5				2	2		2	
6		1		2			1	
7				5			1	
8			1	3				
9				2				
.10	1		1	4	1			
1	1			1		1	2	1
2	1			1				
3							1	1
4	1		1			1		
5			1		1			
6				1			1	
7		1			1			
8	1		1					
9								
.20			1				1	
1			1					
2			1					
3		1					1	1
4			1					
5			1		1		1	
6								
7						1		
8	2		1					1
9	1		2					
.30							1	
1								
2								
3								
4								1
5					1	1		
6								1
7								
8								
9								
.40					1	2		3
.41+								

TABLE X

CALCULATION OF THE AMOUNT OF SOLAR RADIATION PENETRATING THE SEA SURFACE AND OF THE RATE OF EVAPORATION FROM THE SEA

LATITUDE	*BASE*												
	20	*22.5*	*25*	*27.5*	*30*	*32.5*	*35*	*37.5*	*40*	*42.5*	*45*	*47.5*	*50*
Lat. $-35 = x =$	−15	−12.5	−10	−7.5	−5	−2.5	0	2.5	5	7.5	10	12.5	15
Radiation penetrating the water, using f_3 (X) computed from temperature													
$295\,[1 + f_3(x)] = R_p$	355	350	344	334	321	307	295	282	261	239	215	199	194
Back radiation B_r	109	108	107	105	103	101	99	97	93	90	87	84	84
Diff. $= (R_p - B_r)$	246	242	237	229	218	206	196	185	168	149	128	115	110
Expression of rate of heat loss $(R_p - B_r)$ in terms of evaporation, meters per month													
.000517 (Diff.) $= E_c$	.127	.125	.122	.118	.113	.106	.101	.096	.087	.077	.066	.059	.057
Using .2 for Bowen ratio $E_c/1.2$ = corrected evaporation $= E'$	.106	.104	.102	.099	.094	.089	.084	.080	.072	.064	.055	.050	.047
Evaporation according to Wüst { 1920 E_1	.096						.080				.058		.043
Wüst { 1936 E_2	.108		.106		.097		.088		.078		.064		.047
Evaporation according to Cherubim E_3 (1931)	.117						.096				.069		.049
E'/E_1 in per cent	110						105				95		109
E'/E_2 in per cent	98		96		97		98		92		86		100
E'/E_3 in per cent	91						87				80		96
Observed solar radiation on a horizontal surface $= R_s$	379	373	363	345	326	312	304	290	274	260	241	226	216
R_p/R_s in per cent	94	94	95	97	98	98	97	97	95	92	89	88	90

ON THE MUTUAL ADJUSTMENT OF PRESSURE AND VELOCITY DISTRIBUTIONS IN CERTAIN SIMPLE CURRENT SYSTEMS, II

By

C.-G. ROSSBY

Massachusetts Institute of Technology
*and Woods Hole Oceanographic Institution**

In a previous report (Rossby, 1937) the author investigated certain changes in the mass distribution which accompany the slow lateral diffusion of momentum in a straight parallel current in an unlimited ocean of constant depth. The principal results of this investigation may be stated as follows:

The main stream increases slowly in width (for large times (t) it is proportional to $t^{1/4}$) while the maximum velocity in the axis of the current gradually decreases (being proportional to $t^{-1/4}$ for large values of t). If no frictional losses occur at the bottom the total *absolute* momentum of the current remains constant. The diffusion is accompanied by a slight banking to the right of the down stream direction, in such a fashion that the difference in height of the free surface between the right and the left edges of the current eventually increases by about eight per cent. Weak counter currents develop on both sides of the main stream as a result of the banking.

This analysis of the disintegration of a current system is supplemented in the present article with a study of the mutual adjustment of mass and velocity distributions in a current system which is gradually being built up by a prescribed wind system acting upon a portion of the ocean surface. The problem will be analyzed in several stages, to bring out more clearly the mechanics of the adjustment process. Frictional forces resulting from lateral mixing will be neglected in the present study but will be included in a third article to be published in a later issue of this journal.

We shall consider at first a homogeneous, incompressible ocean of constant depth D_o, which is at rest initially. Through wind action a certain amount of momentum is communicated to an infinite strip of the width $2a$. The details of the mechanism of this transfer are not important in the present connection. It is sufficient to say that the fluid column between $y = +a$ and $y = -a$ is endowed with a certain mean velocity u in the positive x-direction. The y-direction is horizontal, normal to the x-direction and points to the left from the x-direction. The momentum relative to the surface of the earth per unit length of current is then given by the expression $2\rho u_o a D_o$, ρ being the density of the water.

* Contribution No. 185.

This momentum (M) is associated with a Coriolis' force of the magnitude fM and directed 90° to the right of the momentum. In this expression f represents the Coriolis' parameter. As no balancing pressure gradient exists, the current will move to the right until enough of a pressure gradient has been established to check further deflection. It is the purpose of this first preliminary calculation to determine the characteristics of the final equilibrium state.

Frictional forces resulting from lateral mixing will be neglected outside the main stream. Within the stream they are assumed to maintain a laterally constant axial velocity which, however, as a result of the displacement of the current to the right must decrease during the adjustment. Since, the lateral stresses merely bring about a redistribution, not a change, of the absolute momentum, the permissibility of the above assumptions depends upon whether a significant redistribution occurs within the interval required for the adjustment process here considered. This question will be considered later.

The general character of the adjustment process is indicated by the cross section in Fig. 84, which is drawn to facilitate the understanding of the analysis but does not correspond to any actual numerical solution. If one assumes that the velocity distribution across the main stream is constant after completed adjustment, it follows that the free surface in the final equilibrium must have a constant slope within the current itself.

During the adjustment the individual fluid columns to the left of the main current shrink vertically, stretch horizontally. Let y_o represent the initial position of a given fluid vertical to the left of the main stream, y its final position. The equation of motion for the x-direction (current axis) takes the form

$$\frac{du}{dt} = fv, \tag{1}$$

there being no pressure gradient in the x-direction and no frictional force. Integration gives

$$u = f(y - y_o) = -f(y_o - y), \tag{2}$$

indicating that each fluid column on completed adjustment will move upstream at a speed proportional to its total displacement to the right.

If the final depth of a certain column is indicated by D, its initial depth by D_o, the equation of continuity takes the form

$$Ddy = D_o dy_o \tag{3}$$

or

$$D = D_o \frac{dy_o}{dy}. \tag{4}$$

After completed adjustment gradient motion prevails. Thus

$$O = -fu - g\frac{dD}{dy}. \tag{5}$$

Combination of (2), (4) and (5) gives

$$\frac{d^2y_o}{dy^2} = \frac{y_o - y}{\lambda^2}, \tag{6}$$

where

$$\lambda = \frac{1}{f}\sqrt{gD_o}. \tag{7}$$

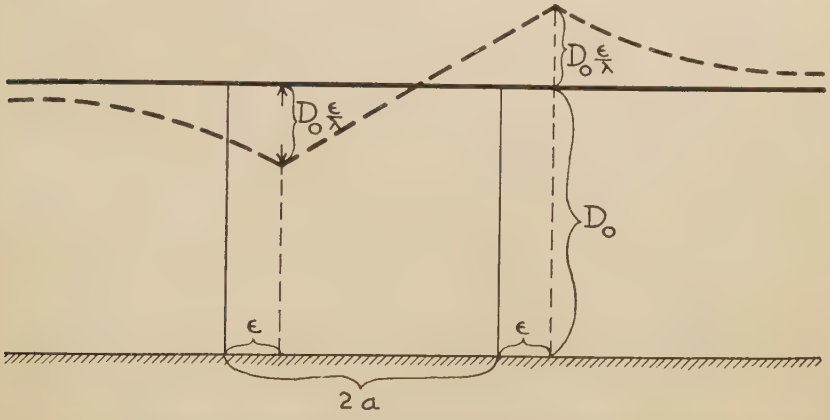

Figure 84. Schematic representation of the adjustment of mass distribution in a homogeneous ocean. See text.

A similar differential equation may be obtained for D,

$$\frac{d^2D}{dy^2} = \frac{D - D_o}{\lambda^2}, \tag{8}$$

and this equation is a special case of a more general equation

$$\frac{\partial^2 D}{\partial x^2} + \frac{\partial^2 D}{\partial y^2} = \frac{D - D_o}{\lambda^2}, \tag{9}$$

valid for arbitrary quasistatic transformations of an originally motionless incompressible fluid sheet of the initial depth D_o.* This last equation expresses the conservation of absolute vorticity.

* The term quasistatic transformation is employed here in preference to the term adiabatic transformation which is generally used in Mechanics to designate processes of this type but which would be ambiguous in meteorology and also to some extent

The length λ is a fundamental parameter in all quasistatic deformations. It is possible to define such a length also for stratified and compressible media, such as the atmosphere. In view of its great significance it seems appropriate to introduce a special name for this quantity. Its magnitude is that of the radius of the inertia circle corresponding to the velocity of long waves in a channel of the depth D_o. It is proposed to name λ the *radius of deformation.*

Integration of (6) gives

$$y_o - y = Ae^{\frac{y}{\lambda}} + Be^{-\frac{y}{\lambda}}, \tag{10}$$

A and B being arbitrary constants of integration. Since the displacement $y_o - y$ must vanish at great distances to the left from the main current (large y-values), it follows that

$$A = 0 \tag{11}$$

and thus

$$y_o - y = \varepsilon e^{-\frac{y}{\lambda}}, \tag{12}$$

ε being the total displacement to the right, of the left edge of the main stream. In this formula the y-coordinate is counted from the final position of the left edge of the main stream.

The depth of the free surface at the left edge of the current (D_l) is given by (4) and (12),

$$D_l = D_o\left(1 - \frac{\varepsilon}{\lambda}\right). \tag{13}$$

By a similar analysis it is possible to compute the rise of the free surface along the right edge of the current for an equal displacement ε to the right. The result is

$$D_r = D_o\left(1 + \frac{\varepsilon}{\lambda}\right). \tag{14}$$

The slope of the free surface across the main stream is now given by $\frac{1}{2a}(D_r - D_l)$. Thus, since gradient wind must prevail in the final equilibrium, it follows that the final mean velocity u_f of the main stream must be given by

$$u_f = \frac{g}{f}\frac{1}{2a}(D_r - D_l) = \frac{gD_o\varepsilon}{f\lambda a} = \frac{\lambda}{a}f\varepsilon. \tag{15}$$

---

in oceanography (for a definition and discussion of adiabatic transformations see for instance, A. Sommerfeld, Atombau und Spektrallinien, 3. Auflage, Vieweg, Braunschweig, 1922).

The displacement of the main stream cannot have changed its absolute momentum. This constancy is expressed by an equation derived previously (Rossby, 1937, p. 19)

$$\int_{-a+\epsilon}^{+a+\epsilon} D_o\,(u_o - fy)\,dy = \int_{-a}^{+a} D\,(u_f - fy)\,dy, \tag{16}$$

the y-coordinate on both sides of the equation being counted from the final center of the current.* Since u_o, u_f, and D_o are constants, it follows that

$$2aD_o u_o = u_f \int_{-a}^{+a} D dy + f \int_{-a+\epsilon}^{a+\epsilon} D_o y dy - f \int_{-a}^{+a} D y dy. \tag{17}$$

The first integral on the left side gives the volume, which remains constant and equal to $2aD_o$. Thus

$$2aD_o\,(u_o - u_f) = fD_o \int_{-a+\epsilon}^{a+\epsilon} y dy - f \int_{-a}^{+a} D y dy. \tag{18}$$

The appropriate expression for D is obtained from (13) and (14). It has the form

$$D - D_o = - D_o \cdot \frac{\varepsilon}{\lambda} \frac{y}{a}. \tag{19}$$

If this expression is substituted in (18) one finds, after some reductions,

$$u_f = u_o - f\varepsilon\left(1 + \frac{a}{3\lambda}\right). \tag{20}$$

* It is of course possible to treat the adjustment of the main stream by the same exact method which was used above in treating the environment. For the main stream, equation (2) changes into

$$u = u_o - f\,(y_o - y) \tag{2a}$$

and the differential equation (6) into

$$\frac{d^2 y_o}{dy^2} = \frac{1}{\lambda^2}\left(y_o - y - \frac{u_o}{f}\right). \tag{6a}$$

The solution of this differential equation is

$$y_o - y = \frac{u_o}{f} + Ae^{\frac{y}{\lambda}} + Be^{-\frac{y}{\lambda}}, \tag{10a}$$

the two integrations constants A and B being needed to satisfy the requirement of continuity in displacement at the two boundaries. The over-all method used above is, however, amply sufficient for our present needs.

It is easy to verify that the product $\varepsilon\left(1+\frac{a}{3\lambda}\right)$ represents the total displacement to the right of the mass center of the current during the adjustment. If (15) and (20) are combined it follows that

$$\varepsilon = \frac{u_o}{f}\frac{1}{1+\lambda/a+a/3\lambda} \tag{21}$$

and, from (15) and (21),

$$u_f = u_o\frac{\lambda/a}{1+\lambda/a+a/3\lambda}. \tag{22}$$

In middle latitudes ($f = 10^{-4}$sec.$^{-1}$) the radius of deformation has a value of 1400 km. for a basin of 2 km. depth. If the current has a width of 200 km. ($a = 100$ km.) and an initial velocity of 50 cm. p. s. it follows that a displacement of one third of one kilometer would be sufficient to establish the required balancing pressure gradient. The initial velocity would be reduced by seven percent as a result of the deflection and the maximum counter current velocity on both sides of the main stream would be about 3.3 cm. p. s.

By the time the main stream reaches its equilibrium position it has acquired a finite velocity to the right and must therefore continue its displacement beyond the equilibrium point until an excessive pressure gradient develops which forces it back. An *inertia* oscillation around the equilibrium position results. It is well known that the period of such an oscillation must be half the pendulum day. The main stream will therefore reach the equilibrium position already in a few hours. From the rapidity of this adjustment it follows that large unbalanced momenta never have time to accumulate. It is probably more correct to assume that the momentum is added quasistatically, in such a fashion that each infinitesimal amount of momentum leads to a practically instantaneous adjustment of the mass distribution. Since a normal wind stress of, say, 1 dyne per cm.^{2} acting on top of a 2 km. deep water column produces a mean momentum per unit mass of less than 0.5 cm. p. s. per day it would appear that the assumption of quasistatic adjustment must be very nearly fulfilled. However, as long as the addition of momentum takes place at a variable and finite rate, a certain fraction of the energy communicated to the system will presumably always appear as an inertia oscillation. The preceding result, that changes in the stress distribution on the ocean surface necessarily must lead to inertia oscillations, was clearly recognized by Ekman in his early studies of drift currents (Ekman, 1905).

It is evident that while the frictional redistribution of momentum during the period of one inertia oscillation may be quite negligible, the total time required for the building up, through wind action, of a gradient current of

the magnitude assumed above is so long that it certainly would be utterly impermissible to neglect the diffusion of momentum during this entire period.

It is next desired to investigate the effect of stratification on the process of mass adjustment. A simple case will be analyzed to bring out the nature of the modification which has to be made in the preceding analysis.

Fig. 85 is a schematic representation of the adjustment process in a two-layer ocean, the upper layer having the density ρ, the lower the density ρ'. The undisturbed thicknesses of the two layers is D_o and D_o'. It is now assumed that an infinitely long strip of the upper fluid, enclosed between the limits $y_o = a$ and $y_o = -a$, is endowed with a velocity u_o. A deflection of the current results and continues until a balancing pressure gradient has been established across the main stream.

The pressure gradients which develop in the upper layer during the adjustment must set the lower homogeneous layer in motion. However, if the latter is very deep it is possible to demonstrate that its displacements and final velocities must be fairly small. It is possible to analyze exactly the adjustment of the lower layer using the method which was applied above to the environment of the main stream in the single-layer case. This will be done later on. As a first approximation, however, it is sufficient to assume that the lower layer remains at rest; thus the deep water displacements associated with deformations of the internal boundary lead to negligibly small axial velocities. This restriction will be removed later.

If the bottom remains at rest it follows that

$$\rho D + \rho' D' = \text{constant} \tag{23}$$

and consequently

$$\frac{d}{dy}(D + D') = \frac{\rho' - \rho}{\rho'}\frac{dD}{dy} = -\frac{\rho' - \rho}{\rho}\frac{dD'}{dy}. \tag{24}$$

It is evident from (23) and (24) that the slope of the internal boundary is always proportional and opposite to the slope of the free surface, which is given by the left side in (24). The preceding analysis, including equations (2), (3) and (4), remains unchanged. The gradient current equation (5) changes into

$$O = -fu - g\frac{d}{dy}(D + D') \tag{25}$$

or, because of (24),

$$O = -fu - g \cdot \frac{\rho' - \rho}{\rho'}\frac{dD}{dy}. \tag{26}$$

Thus, if one reduces the acceleration of gravity in the proportion $\frac{\rho' - \rho}{\rho'}$ and substitutes for g a value γ, defined by

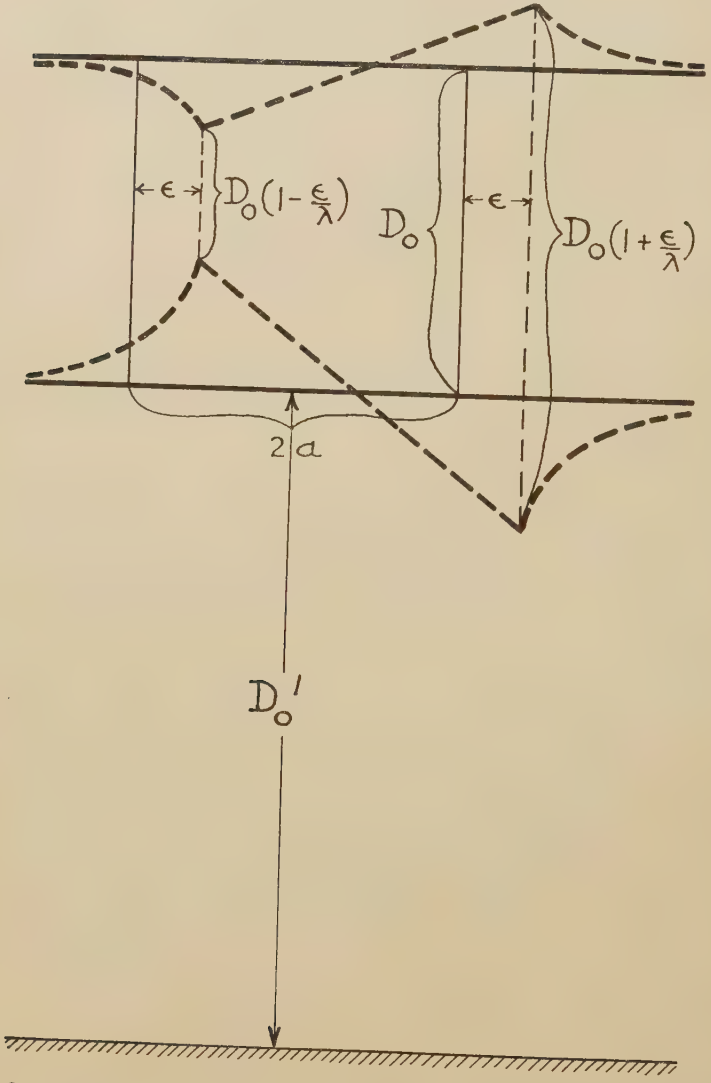

Figure 85. Schematic representation of the adjustment of mass distribution in a double layer ocean. See text.

(27) $$\gamma = g \cdot \frac{\rho' - \rho}{\rho'}$$

all the previously derived results remain valid. The system is in every respect identical with a single-layer ocean of the depth D and subject to an acceleration of gravity of the value γ. The substitution (27) has one very important consequence. The radius of deformation, defined in (7), is now given by

(28) $$\lambda = \frac{1}{f}\sqrt{\gamma D_o} = \frac{1}{f}\sqrt{\frac{\rho' - \rho}{\rho'} g D_o}.$$

Assuming an upper homogeneous layer with an original depth $D_o = 400$ m, and assuming a density discontinuity of 0.2 percent, it follows that

$$\lambda = 28 \text{ km.} \qquad (f = 10^{-4}\text{sec.}^{-1}).$$

The radius of deformation is thus reduced to $\frac{1}{50}$ of its original value. Assuming the same values for u and a as before, the deflection of the current will now be about 2 km. compared with the previous value of 0.33 km. The reduction in the mean speed of the current due to this deflection is greatly increased, the final axial velocity u_f having a value of about 5.3 cm. p. s. and the counter currents are correspondingly increased to about 20 cm. p. s. The radius of deformation measures that distance from either edge of the main stream in which the counter current velocity has fallen off to the fraction $\frac{1}{e}$ of its maximum value, and this distance is now reduced to $\frac{1}{50}$ of its previous value. Thus the adjustment of the mass distribution will be accompanied by the development of strong and narrow counter currents, while the corresponding currents in the homogeneous case will be very broad and extremely weak.

The preceding results suggest that the adjustment of the mass distribution in a stratified medium will be accompanied by a more intense development of inertia oscillations than the corresponding adjustment in a homogeneous medium. It is actually possible to compute the energy available for inertia oscillations by forming the difference between the total energy before and after adjustment. Such a calculation is easily made and clearly indicates that a much larger fraction of the initial energy goes into the oscillating motion in the stratified case than in the homogeneous.

It is found that the initial energy E_o, given by the expression

$$E_o = \rho a D_o \cdot u_o^2,$$

and the final energy E_f are related through the formula

$$E_f = E_o \cdot \frac{\frac{\lambda}{a}}{1 + \frac{\lambda}{a} + \frac{a}{3\lambda}} \tag{29a}$$

and thus the fraction of the initial energy available for inertia oscillations is given by

$$E_{oscillation} = E_o \frac{1 + \frac{a}{3\lambda}}{1 + \frac{\lambda}{a} + \frac{a}{3\lambda}} . \tag{29b}$$

This last expression is not quite correct, a small error resulting from the assumption that the velocity of the main stream is constant laterally also in the final equilibrium state. This error is not significant in the single-layer case but may be of some consequence in a stratified medium. A comparison of the two cases discussed above indicates that in the single-layer ocean only 7% of the initial energy goes into inertia oscillations, whereas in the second case the major portion of the initial energy (89%) must appear as an inertia oscillation.

Since most currents are built up through a fairly gradual addition of momentum the numerical values obtained through the suggested application of the energy integral are of small significance. Nevertheless, because of the variability of the surface stresses it appears probable that vigorous inertia oscillations must develop in stratified media and express themselves as a marked intensification of the large-scale horizontal turbulence which must develop due to the dynamic instability of the shearing zones between the current and its surrounding counter currents (Pekeris, 1938). Such intensification would not occur in homogeneous media. This tentative conclusion agrees well with Parr's suggested relationship between lateral mixing and vertical stability (Parr, 1936).

The total amount of momentum received from the wind per unit time is distributed over a much deeper column in the case of a single-layer homogeneous ocean than in the case of stratified water. Thus the initial unbalanced velocity components will be stronger in stratified than in homogeneous water and this fact would further favor the development of lateral turbulence in stratified water.

We shall next consider motions set up in the deeper of the two layers as a result of displacements and mass adjustments in the upper layer. It is assumed that no tangential stresses are transmitted through the boundary between the two strata. Originally the lower layer is at rest and characterized by a constant depth D_o'.

During the adjustment process the internal boundary will be deformed. Since continuity of mass must be preserved it follows that

$$D'dy' = D_o'dy_o', \tag{30}$$

y_o' and y' being the initial and final positions of a given fluid vertical.

The equation of motion for the x-direction is given by

$$\frac{du'}{dt} = fv' \tag{31}$$

or, after integration,

$$u' = f(y' - y_o') = -f(y_o' - y'). \tag{32}$$

It will now be assumed that wind action or other processes have led to the establishment of a known horizontal pressure gradient in the upper layer. The problem is to determine the final velocity u' in the lower layer for prescribed values of the gradient current u in the upper layer.

It is of course possible to assume that an initially unbalanced current component exists in a portion of the upper layer and to solve simultaneously the equations which describe the adjustment processes in the two layers. In this case the adjustment of the mass distribution is accomplished through a transversal circulation which, to an observer looking downstream, takes place in a clock-wise sense (see fig. 85). Such clock-wise circulations have been observed in the California current during periods of acceleration and estimates of their intensity have been made (Sverdrup, 1938). An exact solution of a problem of this type will be presented by Mr. H. Wexler and the author in a later issue of this journal. For the present we shall restrict ourselves to the case of a prescribed pressure distribution, or gradient current system, in the upper layer. If this new pressure distribution in the upper layer is applied quasistatically the solution presented below represents the final equilibrium state. If it is applied suddenly or built up at an irregular rate, inertia oscillations will appear, both above and below, superimposed upon the equilibrium state here computed.

The depth of the upper layer is D. The height of the free surface is given by $D + D'$ and thus

$$u = -\frac{g}{f}\frac{d}{dy'}(D + D'). \tag{33}$$

The gradient current equation for the lower layer takes the form

$$u' = -\frac{g}{\rho' f}\frac{d}{dy'}(\rho D + \rho' D') \tag{34}$$

or

$$u' = \frac{\rho u}{\rho'} - \frac{\gamma}{f}\frac{dD'}{dy'}. \qquad \left(\gamma = \frac{\rho' - \rho}{\rho'}g\right). \tag{35}$$

A combination of (30), (32) and (35) gives

$$\frac{d^2u'}{dy'^2} - \frac{u'}{\lambda'^2} = -\frac{\rho}{\rho'}\frac{u}{\lambda'^2}, \tag{36}$$

the radius of the deformation λ' now being given by

$$\lambda' = \frac{1}{f}\sqrt{\gamma D_o'} = \frac{1}{f}\sqrt{\frac{\rho' - \rho}{\rho'} g D_o'}. \tag{37}$$

If the superimposed gradient current u vanishes for $y' = \pm\infty$ the same must apply to u'. It then follows from (36) that u' becomes vanishingly small for very large values of λ' (great depths of the lower layer).

The deformation of the internal boundary is easily computed from (30) and (32), combined into the form

$$\frac{D' - D_o'}{D_o'} = -\frac{1}{f}\frac{du'}{dy'}, \tag{38}$$

which is an expression for the conservation of absolute vorticity in the lower layer.

If it is assumed that the upper layer was at rest before the wind stresses responsible for the gradient current u were applied, it follows that the distortion of the free surface, $h = D + D' - D_o - D_o'$, must vanish for large positive and negative values of y. Thus it follows from (33) that u must satisfy the requirement

$$\int_{-\infty}^{+\infty} u dy' = 0. \tag{33b}$$

If the superimposed current is symmetric with respect to y it further follows that one must have

$$\int_{o}^{\infty} u dy' = \int_{-\infty}^{o} u dy' = 0. \tag{33c}$$

One must furthermore assume that the deformation of the free surface took place in such a fashion that no mass was added or subtracted. It follows that one must require that

$$\int_{-\infty}^{+\infty} h dy' = \int_{-\infty}^{+\infty} (D + D' - D_o - D_o')\, dy' = 0. \tag{33d}$$

This last condition is satisfied if u is symmetric and satisfies the condition (33c).

Fig. 86 represents two velocity distributions, u and u', which satisfy equation (36). The velocity distribution in the upper layer, supposedly established through wind action, is given by

$$(39) \qquad \frac{u}{u_m} = \left[1 - \frac{2\beta\,(1+12\beta)\,\eta^2}{1+6\beta} + \frac{8\beta^3\eta^4}{1+6\eta}\right] e^{-\beta\eta^2}, \quad (\lambda'\eta = y')$$

and the corresponding velocity distribution in the lower layer is then

$$(40) \qquad \frac{u'}{u_m} = \frac{\rho}{\rho'}\frac{1}{1+6\beta}\,[1 - 2\beta\eta^2]\,e^{-\beta\eta^2}.$$

In plotting the curves for $\frac{u'}{u_m}$ and $\frac{u}{u_m}$ it was assumed that $\beta = \frac{1}{9}$.

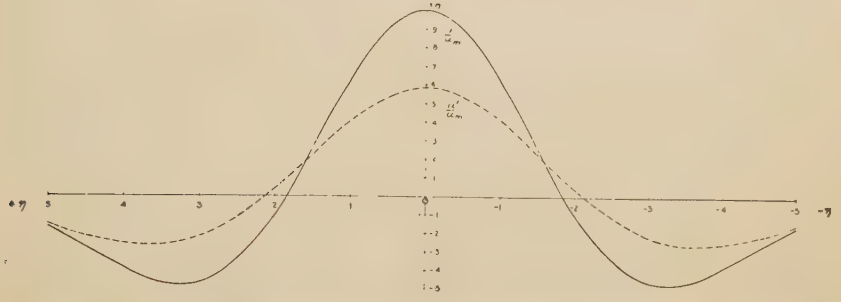

Figure 86. Example of two velocity distributions satisfying equation (36). See text.

The deformation of the internal boundary is represented in Fig. 87. It follows from (38) that the deflections of the internal boundary will be antisymmetric with respect to y'. In the particular case here investigated the equation for the internal boundary is

$$(41) \qquad \frac{D' - D_o'}{D_o'} = \frac{\rho}{\rho'} \cdot \frac{u_m}{f\lambda'} \cdot \frac{2\beta}{1+6\beta}\,[3 - 2\beta\eta^2]\cdot\eta\cdot e^{-\beta\eta^2}$$

It is apparent from the solution presented above that the internal boundary adjusts itself so as to counteract, in the lower layer, the horizontal pressure gradients transmitted downward from the upper layer, *but it is also evident that this compensation is very incomplete.*

The preceding analysis raises several interesting questions. Most important of these is the following: Will the effect of deformations of the free surface be felt to some extent throughout the entire water column also in case of a continuous variation of density with depth or will the dynamically created solenoids in the interior completely cancel the effect of the surface pressure gradient? It is evident that the usefulness of "dynamic" velocity calculations of non-permanent current patterns to a very large extent depends upon the answer to this question.

We shall attempt to answer this question by a study of the following problem:

An ocean basin of uniform depth is at rest initially. The density decreases at a constant rate upward, from the value ρ_b at the bottom to the value ρ_h at the height h_o above the bottom. Above this stable layer there is a homogeneous layer of the density ρ_h. Through wind action, or in some other fashion, the free surface is deformed, and a corresponding system of gradient currents set up in the homogeneous water. How do the deep layers react to the new pressure gradients transmitted from above?

We shall assume that the deep water is made up of a very large number of layers of infinitesimal thickness, each one limited above and below by a surface of constant density. Thus each particular layer is enclosed between two isopycnic surfaces, ρ = constant and $\rho + \delta\rho$ = constant. Within each layer the density may be considered constant and equal to the mean density of the layer $(\rho + \frac{1}{2}\delta\rho)$. Each layer is horizontal before the deformation sets in but is warped during the adjustment process. In the final equilibrium

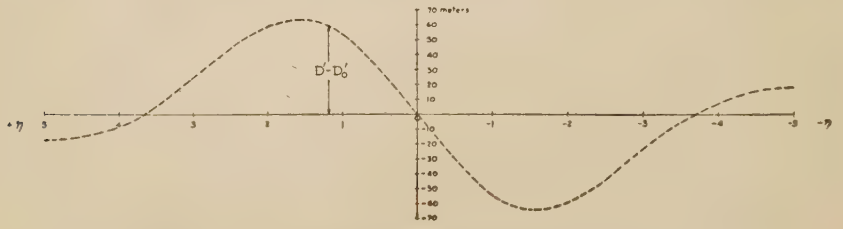

Figure 87. Deformation of the internal boundary. See text.

state *horizontal* gradient flow prevails and the motion is thus parallel to the contour lines for that particular layer.

Now consider a chain of particles in one of these isopycnic layers. In the final stage its circulation may be computed from the circulation theorem which, in this particular case, takes the form

$$C = -f(A - A_o), \tag{42}$$

A_o being the area enclosed by the projection of the chain on a level surface before the deformation, A the corresponding area after the deformation. C is positive for cyclonic circulation.

In the final state horizontal gradient motion prevails. Thus

$$C = \oint u\delta x + v\delta y \tag{43}$$

δx and δy being the components of the horizontal projections of the line elements of the chain. It follows from Stokes' theorem that

$$C = \int\int \left(\frac{\partial v}{\partial x} - \frac{\partial u}{\partial y}\right)\delta x\delta y \tag{44}$$

where $\frac{\partial}{\partial x}, \frac{\partial}{\partial y}$ *now represent derivatives with respect to* x *and* y *along a constant density surface.*

The right side of equation (42) can be written in the form

$$-f\left[\int\int \delta x \delta y - \int\int \delta x_o \delta y_o\right], \tag{45}$$

the subscript 0 referring to the initial state. The equation of continuity gives

$$D = D_o \frac{\partial (x_o, y_o)}{\partial (x, y)} \tag{46}$$

D_o and D representing the vertical thickness of an individual element before and after the deformation. Thus

$$f(A - A_o) = f\int\int\left[1 - \frac{\partial (x_o, y_o)}{\partial (x, y)}\right]\delta x \delta y = f\int\int \frac{D_o - D}{D_o}\delta x \delta y \tag{47}$$

and consequently,

$$\zeta = \frac{\partial v}{\partial x} - \frac{\partial u}{\partial y} = f\frac{D - D_o}{D_o}. \tag{48}$$

ζ is the vertical component of vorticity in the particular isopycnic sheet under study. *In the equation (48)* $\frac{\partial}{\partial x}$ *and* $\frac{\partial}{\partial y}$ *represent derivatives with respect to* x *and* y *along a surface of constant density.*

If $z\ (x, y, \rho)$ represents the height of a given isopycnic surface after adjustment, $z_o\ (\rho)$ its initial height, it follows that

$$D = -\frac{\partial z}{\partial \rho}\delta\rho, \quad D_o = -\frac{\partial z_o}{\partial \rho}\delta\rho \tag{49}$$

and thus

$$\zeta = \frac{\partial v}{\partial x} - \frac{\partial u}{\partial y} = f\frac{\frac{\partial z}{\partial \rho} - \frac{\partial z_o}{\partial \rho}}{\frac{\partial z_o}{\partial \rho}}. \tag{50}$$

If one introduces a new measure for the density, defined by

$$r = \frac{\rho_b - \rho}{\rho_b - \rho_h}, \quad \rho_b - \rho_h = 2\kappa\rho_b, \quad \rho = \rho_b(1 - 2\kappa r) \tag{51}$$

it follows that

$$z_o = 0,\ z = 0,\ r = 0 \text{ for } \rho = \rho_b \tag{52}$$

$$z_o = h_o,\ z = h,\ r = 1 \text{ for } \rho = \rho_h. \tag{53}$$

The assumption is now introduced that the initial vertical density distribution is linear. Thus

$$z_o = h_o r. \tag{54}$$

Substitution in (50) gives

$$\zeta = \frac{\partial v}{\partial x} - \frac{\partial u}{\partial y} = f \frac{\dfrac{\partial z}{\partial r} - h_o}{h_o}. \tag{55}$$

If one finally introduces the symbol Δ for the vertical departure of each isopycnic surface from its initial position, the law for the conservation of vorticity reduces to the form

$$\zeta = \frac{\partial v}{\partial x} - \frac{\partial u}{\partial y} = \frac{f}{h_o} \frac{\partial \Delta}{\partial r}, \quad \Delta = z - h_o r. \tag{56}$$

The hydrostatic equation must be transformed to include r instead of z as the independent variable, since otherwise the law for the conservation of vorticity cannot be effectively utilized. The pressure at a height z above the bottom is given by

$$p = g\rho_h H + g \int_z^h \rho dz, \tag{57}$$

H being the thickness of the superimposed homogeneous layer. Integration by parts gives

$$p = g\rho_h (h + H) - g\rho z - g \int_\rho^{\rho_h} z d\rho \tag{58}$$

or

$$p = g\rho_h (h + H) - g\rho z + 2\kappa g \rho_b \int_r^1 z dr. \tag{59}$$

If n represents one of the horizontal coordinates (x or y) and the variation of p along a constant density surface be computed one finds

$$\frac{\partial p}{\partial n} = g\rho_h \frac{\partial (h + H)}{\partial n} - g\rho \frac{\partial z}{\partial n} + 2\kappa g \rho_b \int_r^1 \frac{\partial z}{\partial n} dr. \tag{60}$$

The horizontal variation of any function p in the n-direction and the variation of p with n along a constant density surface are connected through the formula

$$\frac{\partial p}{\partial n} = \left(\frac{\partial p}{\partial n}\right)_z + \frac{\partial p}{\partial z} \frac{\partial z}{\partial n}. \tag{61}$$

If p represents the pressure the above formula reduces to

$$\frac{\partial p}{\partial n} = \left(\frac{\partial p}{\partial n}\right)_z - g\rho \frac{\partial z}{\partial n}. \tag{62}$$

Thus

$$\left(\frac{\partial p}{\partial n}\right)_z = g\rho_h \frac{\partial}{\partial n}(h + H) + 2\kappa g \rho_b \int_r^1 \frac{\partial z}{\partial n} dr. \tag{63}$$

It follows that gradient current velocities may be computed from

$$\rho f v = g\rho_h \frac{\partial}{\partial x}(h + H) + 2\kappa g \rho_b \int_r^1 \frac{\partial z}{\partial x} dr \tag{64}$$

$$-\rho f u = g\rho_h \frac{\partial}{\partial y}(h + H) + 2\kappa g \rho_b \int_r^1 \frac{\partial z}{\partial y} dr. \tag{65}$$

Disregarding compressibility, the total percentual variation of density along a vertical in the open sea is of the order of magnitude of 0.2 percent. Thus it is entirely permissible to simplify the above equations by setting

$$\frac{\rho_h}{\rho} = \frac{\rho_b}{\rho} = 1. \tag{66}$$

Since z_o is independent of x and y one finally obtains

$$\frac{fv}{g} = \frac{\partial}{\partial x}(h + H) + 2\kappa \int_r^1 \frac{\partial \Delta}{\partial x} dr \tag{67}$$

$$-\frac{fu}{g} = \frac{\partial}{\partial y}(h + H) + 2\kappa \int_r^1 \frac{\partial \Delta}{\partial y} dr \tag{68}$$

and, for the vorticity,

$$\frac{f\zeta}{g} = \left(\frac{\partial^2}{\partial x^2} + \frac{\partial^2}{\partial y^2}\right)(h + H) + 2\kappa \int_r^1 \left(\frac{\partial^2}{\partial x^2} + \frac{\partial^2}{\partial y^2}\right)\Delta dr. \tag{69}$$

The vertical variation of vorticity is obtained from (69) through differentiation. The result is

$$\frac{\partial \zeta}{\partial r} = -\frac{2\kappa g}{f}\left(\frac{\partial^2}{\partial x^2} + \frac{\partial^2}{\partial y^2}\right)\Delta. \tag{70}$$

Eliminating ζ between (56) and (70) one obtains

$$\boxed{\frac{\partial^2 \Delta}{\partial r^2} + \frac{2\kappa g h_o}{f^2}\left(\frac{\partial^2 \Delta}{\partial x^2} + \frac{\partial^2 \Delta}{\partial y^2}\right) = 0.} \tag{71}$$

There must be continuity in velocity and consequently also in vorticity at the boundary between the homogeneous and the stable water. It follows

that ζ is prescribed for the upper boundary ($r = 1$). At the bottom $\Delta = 0$. Thus there is one solution, and one only, which satisfies the requirements of the original problem and the fundamental differential equation (71).

In the case of a parallel current system the preceding equations take a very simple form. It follows from (68) that

$$\frac{\partial u}{\partial r} = \frac{2\kappa g}{f}\frac{\partial \Delta}{\partial y} \tag{72}$$

and from (56) that

$$\frac{\partial u}{\partial y} = -\frac{f}{h_o}\frac{\partial \Delta}{\partial r}. \tag{73}$$

If one introduces the radius of deformation λ, defined by

$$\lambda^2 = \frac{2\kappa g h_o}{f^2} \tag{74}$$

it follows that

$$\frac{\partial U}{\partial r} = \frac{\partial Z}{\partial \eta} \tag{75}$$

$$\frac{\partial U}{\partial \eta} = -\frac{\partial Z}{\partial r}\left(y = \lambda\eta,\ U = \frac{u}{f\lambda},\ Z = \frac{\Delta}{h_o}\right). \tag{76}$$

Thus U and Z are conjugate functions, satisfying the equations

$$\left(\frac{\partial^2}{\partial r^2} + \frac{\partial^2}{\partial \eta^2}\right)U = 0,\ \left(\frac{\partial^2}{\partial r^2} + \frac{\partial^2}{\partial \eta^2}\right)Z = 0. \tag{77}$$

The boundary conditions are:

$$Z = 0 \text{ for } r = 0. \tag{78}$$

$$U \text{ prescribed for } r = 1. \tag{79}$$

The rate at which the current velocity decreases downward is well illustrated by the following case:

The superimposed velocity in the homogeneous layer is given by

$$u_{hom} = u_m \cos k\eta \tag{80}$$

This represents a system of parallel currents of alternating direction, the "wave-length" L being given by

$$L = \frac{2\pi\lambda}{k},\ k = \frac{2\pi\lambda}{L}. \tag{81}$$

The corresponding velocity distribution in the interior is given by

$$u = u_m \cdot \frac{e^{kr} + e^{-kr}}{e^k + e^{-k}} \cos k\eta, \tag{82}$$

and the deformation of the individual density surfaces may be computed from

$$\Delta = \frac{h_o}{f\lambda} u_m \cdot \frac{e^{kr} - e^{-kr}}{e^k + e^{-k}} \sin k\eta. \tag{83}$$

The velocity at the bottom (u_b) is given by

$$\frac{u_b}{u_m} = \frac{\cos k\eta}{\cosh k} \tag{84}$$

and the maximum bottom velocity by

$$\frac{u_{b\,max}}{u_m} = \frac{1}{\cosh k} = \frac{1}{\cosh \frac{2\pi\lambda}{L}} \tag{85}$$

Thus the effect of the superimposed velocity gradients will extend to greater depths or, which is the same, be more marked at the same depth for a longer "wave-length" L than for a shorter.

The ratio (85) between the maximum bottom velocity and the maximum gradient current velocity has been computed for different values of $n = \frac{L}{\lambda}$. Assuming $h_o = 1800$ m., $2\kappa = 2 \cdot 10^{-3}$, $g = 10^3$ cm. sec.$^{-2}$, $f = 10^{-4}$ sec.$^{-1}$, one finds

$$\lambda = 60 \text{ km.}$$

The resulting values are given in the line marked $\frac{K_o}{h_o} = 0$ in table I.

It is evident from these values that the redistribution of mass within a single 1800 m. deep layer of uniform stability is insufficient to reduce a superimposed horizontal surface pressure gradient to zero at the bottom It appears that for a current width of 240 km. ($L = 480$ km., $n = 8$) the maximum bottom velocity will still be 75% of the maximum gradient velocity of the surface layer. If the total density range and the depth of the stable layer are doubled the value of λ is doubled. The appropriate value of n is reduced to 4, but the maximum bottom velocity is still 40% of the maximum surface velocity. There is no reason to expect such high velocities near the bottom and thus the question concerning the equalization of the horizontal pressure gradients at great depths remains open.

In a further effort to settle this question we shall finally investigate if the presence of another, deep homogeneous layer below the stable water plays

an important role in the cancellation of surface pressure gradients through redistribution of mass. It will be assumed that the deep water has a constant density ρ_b and an undisturbed depth K_o. Then, if Δ_o represents the deformation of the surface separating the lower homogeneous layer from the stable water above, it follows from the conservation of vorticity in the lower layer and from the requirement of continuity in the velocity distribution that

$$\left(\frac{\partial u}{\partial y}\right)_{r=0} = -\frac{f\Delta_o}{K_o} \tag{88}$$

or,

$$\left(\frac{\partial U}{\partial \eta}\right)_{r=0} = -\frac{h_o}{K_o} \cdot Z_{r=0}. \tag{89}$$

The solution corresponding to the boundary condition (80) and the revised boundary condition (89) is

$$\frac{u}{u_m} = \frac{h_o \cosh kr + kK_o \sinh kr}{h_o \cosh k + kK_o \sinh k} \cos k\eta \tag{90}$$

and

$$\frac{\Delta}{h_o} = \frac{u_m}{f\lambda} \frac{h_o \sinh kr + kK_o \cosh kr}{h_o \cosh k + kK_o \sinh k} \sin k\eta. \tag{91}$$

For $K_o = 0$ these equations become identical with (82) and (83) and for $K_o \to \infty$ the solution reduces to

$$\frac{u}{u_m} = \frac{\sinh kr}{\sinh k} \cos k\eta \tag{92}$$

$$\frac{\Delta}{h_o} = \frac{u_m}{f\lambda} \frac{\cosh kr}{\sinh k} \sin k\eta. \tag{93}$$

The relation between the maximum velocity in the homogeneous bottom layer and the maximum velocity in the homogeneous surface layer is now obtained by setting $r = 0$ in (90). The result is

$$\frac{u_{b\ max}}{u_m} = \frac{1}{\cosh k \left(1 + \frac{kK_o}{h_o} \tanh k\right)} = \frac{1}{\cosh \frac{2\pi\lambda}{L} \left(1 + \frac{2\pi\lambda}{L} \cdot \frac{K_o}{h_o} \tanh \frac{2\pi\lambda}{L}\right)}. \tag{94}$$

For $K_o = 0$ this formula reduces to the one derived previously (85) and for $K_o \to \infty$ the ratio becomes zero, i. e. the bottom layer will then be at

rest. For an initial depth of the lower homogeneous layer of 1800 m. and for the same value of n as before ($n = 8$, $L = 480$ km.) the maximum bottom velocity will still be 50% of the maximum gradient velocity in the upper layer.

TABLE I

$\frac{K_o}{h_o}$ \ n	0.5	1	2	4	8	16
0	.0000	.0037	.0862	.399	.755	.928
0.5	.0000	.0009	.0337	.232	.605	.855
1	.0000	.0005	.0277	.162	.499	.809
2	.0000	.0003	.0119	.103	.372	.774
∞	0	0	0	0	0	0

The preceding analysis indicates that the effect on the deep water of pressure gradients transmitted from above will be considerably reduced through redistribution of mass in the interior of the ocean, but with reasonable values for the depth and for the total vertical density range there is always a considerable residual effect even in the homogeneous bottom layer. One must conclude that a changing pressure applied on a horizontal surface near the sea surface will be felt also in the bottom water and thus must produce, at least temporarily, sizeable stratospheric currents.

It is obvious that this conclusion does not apply to cases of steady state motion in the ocean, since various frictional forces then have the opportunity to dissipate the kinetic energy of the stratospheric currents. However, the so-called permanent wind systems which actuate the superficial layers of the ocean are changing from day to day and from season to season. It is the author's definite opinion that these changing wind systems must produce deformations of the ocean surface and consequently horizontal pressure gradients which, in the light of the preceding analysis, necessarily must set also the deepest strata in motion. There is no justification whatsoever for the point of view which pictures the ocean stratosphere as completely inert apart from the slow thermal circulation produced by the production of bottom water through cooling in the Antarctic.

SUMMARY

The principal purpose of this investigation is to study those changes in the internal mass distribution which accompany the initial establishment of oceanic current systems through wind stresses applied at the sea surface. Whenever surface water is set in motion through wind action, horizontal pressure gradients are established in the uppermost layers of the ocean. Surrounding and underlying water masses which are not acted upon by the wind, will be set in motion by these new pressures. If, as a first approximation, frictional forces are neglected outside the body of water which is directly influenced by the wind, the displacements and final equilibrium of the surrounding masses may be determined from the requirement that each individual element of water must retain its absolute vorticity. The final equilibrium thus determined is one of dynamic equilibrium, i.e. characterized by steady motion.

The total energy (potential and kinetic) of the final equilibrium is normally less than the initial energy (kinetic energy received from the wind). The difference goes into inertia oscillations around the final equilibrium state computed from the vorticity theorem mentioned above.

The specific results may be stated as follows:

1. If, through wind action, an infinite strip of water in an initially motionless homogeneous ocean basin is set in motion in the direction of its own axis, the entire current filament will be deflected to the right of the downstream direction* as a result of the initially unbalanced Coriolis' force associated with its momentum. The sea surface will rise along the right edge, fall along the left edge, until a transversal pressure gradient (slope) is established which exactly balances the Coriolis' force. The rise (drop) of the sea surface in the environment of the current may be computed from the requirement that each vertical column of water must conserve its absolute vorticity.

2. The sum of the potential and kinetic energy in this equilibrium state is somewhat less than the initial kinetic energy of the system (there is no potential energy in the initial state). The difference in energy goes into an inertia oscillation with a period of twelve pendulum hours. As a result of this inertia oscillation the deflection of the current will proceed beyond the equilibrium position and then reverse direction. However, in a homogeneous ocean the fraction of energy stored in this inertia oscillation is small.

3. If, through wind action, an infinite strip of water in the upper of two homogeneous layers is set in motion in the direction of its own axis, a similar adjustment process occurs. While the free surface rises along the right edge, sinks along the left edge of the current, the internal boundary

* On the northern hemisphere.

will be deformed in the opposite sense. If the lower layer is very deep it is permissible to assume that it will be practically motionless also after completed adjustment. The ratio of the deformation of the free surface to that of the internal boundary then has the same value as the ratio of the difference in density between the two layers to the density of the upper layer. In this case the total deflection of the current system is increased several times over the corresponding deflection in a homogeneous ocean.

4. In such a double-layer ocean with a resting bottom layer the fraction of the initial energy which goes into inertia oscillations is many times larger than in a homogeneous ocean.

5. The adjustment to equilibrium of the initially unbalanced current filament is in both cases accompanied by the development of counter currents in the environment. These counter currents are very weak and broad in the case of a homogeneous ocean but narrow and intense in the case of a double-layer ocean.

6. The shear zones between the current and its environment are known to be dynamically unstable and should therefore have a tendency to break up into large-scale horizontal eddies (lateral turbulence).

7. Since there is a much greater supply of energy available for vigorous inertia oscillations in a double-layer ocean than in a homogeneous ocean, it is reasonable to assume that lateral turbulence must be more strongly developed in stratified than in homogeneous water; this conclusion strongly supports Parr's suggestion concerning the relation between lateral eddy viscosity and vertical stability.

8. In a stratified ocean the momentum received from the wind will be distributed over a shallow vertical column, whereas it will be spread over a much deeper column in homogeneous water. For this reason strong unbalanced current components are more likely to occur in stratified than in homogeneous water. This would tend to produce stronger inertia oscillations, and hence presumably stronger lateral turbulence, in stratified water than in homogeneous, again in agreement with the suggested relationship between lateral turbulence and vertical stability.

9. If the lower of the two layers in the idealized ocean referred to above has a finite depth, the displacement of the upper unbalanced current towards its equilibrium position will be accompanied by a transversal displacement of the lower layer in the opposite direction. This displacement below will, as a result of the Coriolis' acceleration, lead to the development of a gradient current in the lower layer in the same direction as the initial current in the upper layer. Thus, although the internal boundary between the two layers is deformed in such a fashion as to counteract the pressure gradients associated with the deformations of the free surface, it may be stated that it is normally impossible to superimpose a horizontal pressure gradient at the

ocean surface without having its effect temporarily transmitted all the way to the bottom layer.

10. This result is further analyzed in the case of an ocean consisting of an upper, homogeneous layer and a lower stable layer with an initially linear density distribution. It is assumed that a prescribed horizontal pressure distribution (perturbation pressure) is established in a geopotential surface within the upper homogeneous layer. Assuming that each infinitesimal isopycnic layer in the stable water conserves its absolute vorticity, it is possible to determine the final equilibrium state. It is found that sizeable gradient currents normally must develop also next to the bottom.

11. The percentual rate at which a prescribed perturbation pressure at the surface is equalized with increasing depth in an ocean basin of normal stability depends upon the lateral dimensions of the superimposed perturbation. A superimposed gradient current system in the upper homogeneous layer with a width of a few kilometers will hardly be felt at the bottom of the stratified layer (assumed to have a depth of 1800 m), but if the superimposed current has a width of between two and three hundred kilometers the horizontal pressure gradient at the bottom will still be about one half of the surface pressure gradient.

12. If there is a deep layer of homogeneous water also below the stable layer the gradient currents next to the bottom will be further reduced, but it still appears that sizeable gradient currents must develop in the bottom water whenever the horizontal pressure distribution in the homogeneous water near the surface changes over reasonably wide areas.

13. The preceding conclusions regarding the motion of the bottom water do *not* apply to a perfectly steady state of motion in the ocean. However, since the large atmospheric wind systems which drive the ocean circulation change from day to day and from season to season it is permissible to state with a reasonable degree of assurance, that it is entirely inappropriate to consider the homogeneous bottom water as inert beyond the slow thermal circulation maintained by antarctic cooling.

14. It is in particular injustifiable to assume à priori that the velocity distribution within larger non-permanent current patterns (such as the larger of those eddies which form intermittently along the edges of the permanent current systems) may be computed on the basis that there is no motion in the deep water.

REFERENCES

1. Ekman, V. W.
1905. On the Influence of the Earth's Rotation on Ocean-Currents, Arkiv. für Matematik, Astronomi och Fysik, Bd. 2, No. 11.
2. Parr, A. E.
1936. On the Probable Relationship between Vertical Stability and Lateral Mixing Processes, Journal du Conseil, Vol. XI, No. 3.
3. Pekeris, C. L.
1938. Wave Disturbances in a Homogeneous Current, Transactions of the American Geographical Union, Vol. XX.
4. Rossby, C.-G.
1937. On the Mutual Adjustment of Pressure and Velocity Distribution in Certain Simple Current Systems, Journal for Marine Research, Vol. I, No. 1.
5. Sverdrup, H. U.
1938. On the Process of Upwelling, Journal for Marine Research, Vol. I, No. 2.

DISCUSSION

LATERAL MIXING AND VERTICAL STABILITY IN THE CARIBBEAN SEA REGION

IN connection with studies of turbulence accompanying fluid motion in the atmosphere and ocean a problem of some prominence concerns the relation between the magnitudes of lateral and vertical turbulent components; an attempt has been made in two recent papers[1] to show that lateral mixing along isopycnal surfaces in the Caribbean Sea region is increased (with an accompanying decrease in vertical turbulence) when the vertical stability of the water column is increased. In support of this concept the qualitative relationship of horizontal distribution of salinity (termed salinity "streakiness") at three levels (salinity maximum: 100–150 meters depth; salinity minimum: average depth 775 meters; 15° isotherm: 200–400 meters depth) in the Caribbean region to vertical stability of the water column was considered, and it was concluded that the greater salinity "streakiness" along the 15° isothermal sheet resulted because its vertical position in the water column was less stable than the positions either of the salinity maxima or salinity minima, as a consequence of which lateral mixing would be relatively less intense. No allowance appears to be given (in the papers referred to in footnote 1) for the possible effect of relative changes in salinity concentration produced by vertical turbulence.

Since this interpretation is contrary to that recently given for an investigation of the same region[2] it seems desirable, in order to avoid possible confusion in the future, to summarize briefly the findings bearing on the problem of the relationship between lateral turbulence and vertical variation of density. The basic data for both investigations (footnotes 2 and 3) are the same ("Atlantis" stations 1499 and 1510). It is proposed to show by means of comparative stability calculations in this area at the depth of the 15° isotherm and at the depth of the salinity minimum concentration, that at the latter level the water instead of being vertically more stable actually possessed only a vertical stability of one fifth to one seventh of

[1] PARR, ALBERT EIDE
1936. On the probable relationship between vertical stability and lateral mixing processes. Jour. du Conseil. Vol. XI, No. 3, pp. 308–313.
1937. A contribution to the hydrography of the Caribbean and Cayman seas. Bull. Bingham Oceanographic Collection. Vol. V, Art. 4, 110 pp.

[2] To be published in Papers in Physical Oceanography and Meteorology under the title: Application of the distribution of oxygen to the physical oceanography of the Caribbean Sea region. Contribution No. 112 from the Woods Hole Oceanographic Institution by H. R. Seiwell.

that at the 15° isotherm. The second consideration involves the values of the second derivatives of the vertical salinity gradients at the levels concerned, because if it is to be granted that an increased vertical stability damps the vertical turbulent component (assuming that other factors tending to create turbulence, such as current velocity, remain constant), it does not necessarily follow, unless the curvatures of the vertical gradients of transferable substances decrease proportionately, that the amount of vertical transfer due to turbulence would likewise decrease. Thus, that vertical transfer of salinity does not appear to decrease inversely proportional to vertical stability for the levels concerned is shown.

At station 1499 the 15° isotherm was found at 260 meters depth; the density (σ_t) at this depth was 26.70. The mean density gradient $\left(\frac{\Delta\sigma_t}{\Delta Z}\right)$ taken over a distance of 100 meters above and below this depth is 5.9×10^{-5} units of σ_t per centimeter. The salinity minimum (34.68 0/00) at this station occurred at 725 meters at which depth the density (σ_t) was 27.32. The mean density gradient $\left(\frac{\Delta\sigma_t}{\Delta Z}\right)$ taken over a distance of 100 meters above and below this depth is 8.0×10^{-6} units of σ_t per centimeter. Thus, the ratio of the density gradients, $\left(\frac{\Delta\sigma_t}{\Delta Z}\right)_{15°} \Big/ \left(\frac{\Delta\sigma_t}{\Delta Z}\right)_{S_{min}}$, is 7.4, or the stability at the depth of the 15° isotherm was more than seven times that at the depth of the salinity minimum concentration.

At station 1510 the 15° isotherm occurred at 290 meters depth; the density (σ_t) at this depth was 26.70. The mean density gradient $\left(\frac{\Delta\sigma_t}{\Delta Z}\right)$ taken over a distance of 100 meters above and below this depth is 4.3×10^{-5} units of σ_t per centimeter. The salinity minimum (34.74 0/00) at this station occurred at 750 meters at which depth the density was 27.36. The mean density gradient $\left(\frac{\Delta\sigma_t}{\Delta Z}\right)$ taken over a distance 100 meters above and below this depth is 8.5×10^{-6} units of σ_t per centimeter. Thus, the ratio of density gradients, $\left(\frac{\Delta\sigma_t}{\Delta Z}\right)_{15°} \Big/ \left(\frac{\Delta\sigma_t}{\Delta Z}\right)_{S_{min}}$, is 5.1, or the stability at depth of the 15° isotherm was more than five times that at the depth of the salinity minimum.

Thus, it appears that, as far as stations 1499 and 1510 are indicative of conditions in the eastern Caribbean,[3] the water column is vertically more

[3] For this purpose, estimation of stability by calculation of $\frac{\Delta\sigma_t}{\Delta Z}$ is sufficiently accurate for the depths concerned. However for accurate values the method of

stable (5 to 7 times) at the depth of the 15° isotherm than at the depth of the minimum salinity concentration[4] and not the reverse as has been utilized to illustrate a relationship between lateral turbulence and vertical stability (referred to in footnote 1).

Consideration of the second derivatives of the vertical salinity gradients for the three levels concerned (determined from the data for stations 1499 and 1510) shows that for any given vertical turbulent coefficient the change in salinity concentration per unit time will be greatest at the depth of the salinity maxima and least at the depth of the 15° isothermal sheet; in fact, at the former level a vertical turbulent coefficient of approximately 1/50th of that acting at the latter level will produce the same time change in concentration. Thus:

$$\text{Salinity maximum:} \frac{\partial^2 s}{\partial Z^2} = -3.3 \times 10^{-11} \text{ g.g.}^{-1} \text{ cm.}^{-2}$$

$$15° \text{ isotherm:} \frac{\partial^2 s}{\partial Z^2} = 7.0 \times 10^{-13} \text{ g.g.}^{-1} \text{ cm.}^{-2}$$

$$\text{Salinity minimum:} \frac{\partial^2 s}{\partial Z^2} = 10.0 \times 10^{-13} \text{ g.g.}^{-1} \text{ cm.}^{-2}$$

In the investigation of the Caribbean Sea region (referred to in footnote 2) it was calculated that the time rate of change of salinity by a lateral eddy diffusing coefficient of 10^5 C.G.S. units would, at mid depths, amount to only about four per cent of that observed. It appears probable that lateral eddy components of a high order of magnitude do exist, but it has not been possible, on the basis of existing information, to isolate the diffusion effects produced by the combined lateral and vertical eddy components and this, together with information presented above, is taken as a basis for suggesting that no satisfactory information is available from the Caribbean area to illustrate that increased lateral diffusion accompanies increased vertical stability.

H. R. Seiwell,

Hesselberg and Sverdrup ("Die Stabilitätsverhältnisse des Seewassers bei vertikalen Verschiebungen," Bergens Museums Aarbok, 1914–15, Nv. 15) should be used.

[4] A calculation of the average values of $\frac{\Delta \sigma_t}{\Delta Z}$ at depths of the 15° isotherm and at depths of the salinity minimum concentration, for the entire Caribbean region, gave as the average approximate stability relationship: $\left(\frac{\Delta \sigma_t}{\Delta Z}\right)_{15°} \Big/ \left(\frac{\Delta \sigma_t}{\Delta Z}\right)_{S_{min}} = 3.2.$

COMMENT

IN reply to the foregoing, it will be sufficient to refer to the complete reconsideration and withdrawal of the use of the Eastern Caribbean Hydrography as a possible illustration of the relationship between vertical stability and lateral mixing, already previously published in a recent report by the writer,[1] which Seiwell completely omits from consideration and from mention in his list of references to the subject of his comments.

A. E. PARR

[1] A. E. Parr: Further Observations on the Hydrography of the Eastern Caribbean and Adjacent Atlantic Waters. Bull. Bingham Oceanogr. Coll. Vol. VI, Art. 4, June 1938.

TABLE OF CONTENTS

Page

1. **C. L. Utterback** and **L. A. Sanderman**: Radium content of some inshore bottom samples in the Pacific Northwest 187
2. **Richard H. Fleming**: Tides and tidal currents in the Gulf of Panama 192
3. **Norris W. Rakestraw** and **Victor M. Emmel**: The relation of dissolved oxygen to nitrogen in some Atlantic waters 207
4. **George F. McEwen**: Some energy relations between the sea surface and the atmosphere 217
5. **C. G. Rossby**: On the mutual adjustment of pressure and velocity distributions in certain simple current systems, II 239
6. *DISCUSSION:* Lateral mixing and vertical stability in the Caribbean Sea region. By H. R. Seiwell. Comment. By A. E. Parr 264